

**VELOCITY-CONTROL PERFORMANCE  
WITH A FINGERTIP CONTROLLED  
ADMITTANCE-TYPE HAPTIC  
DEVICE**

by

Troy K. Arbuckle

A thesis submitted to the faculty of  
The University of Utah  
in partial fulfillment of the requirements for the degree of

Master of Science

Department of Mechanical Engineering

The University of Utah

December 2012

Copyright © Troy K. Arbuckle 2012

All Rights Reserved

THE UNIVERSITY OF UTAH GRADUATE SCHOOL

**STATEMENT OF THESIS APPROVAL**

The thesis of           Troy K. Arbuckle          

has been approved by the following supervisory committee members:

<u>Jake J. Abbott , Chair</u>	<u>October 19, 2012</u> Date Approved
<u>William R. Provancher , Member</u>	<u>October 19, 2012</u> Date Approved
<u>Jonathan E. Butner , Member</u>	<u>October 23, 2012</u> Date Approved

and by           Timothy Ameal          , chair of  
the department of           Mechanical Engineering          

and by Charles A. Wight, Dean of The Graduate School.

## ABSTRACT

Admittance-type robotic devices are commonly used to complete tasks that require a high degree of precision and accuracy because they appear nonbackdrivable to many disturbances from the environment. Admittance-type robots are controlled using admittance control; a human interacts directly with a force sensor mounted to the robot, and the robot is computer-controlled to move in response to the applied force. The experiment herein was conducted to determine under which operating conditions human velocity control is optimized for admittance devices that are controlled under proportional-velocity control, and to determine the degradation in control under nonoptimal conditions. In this study, the desired velocity of the device was shown on a visual display. The desired velocity was shown with a scaling factor from the actual velocity of the device because the device often moved at velocities too slow to perceive visually. The admittance gain,  $k_a$ , desired velocity,  $V_d$ , and the visualization scale factor,  $S$  were tuned to adjust the user's experience when interacting with an admittance device. We found that in velocity-tracking tasks, scaling the visual feedback only has a significant effect on performance for very slow desired velocities (0.1 mm/s), for the range of velocities tested here. In this thesis, we give evidence that there exists a range of velocities and forces within which humans optimally interact with admittance-type devices. We found that the optimal range of velocities is between 0.4 mm/s and 1.0 mm/s, inclusive, and the optimal range of forces is between 0.4 N and 4.0 N, inclusive. To ensure optimal velocity-control performance, the admittance gain should be selected such that the desired velocity and target force remain within their respective optimal ranges simultaneously. We also found that on average subjects moved faster than the desired velocity when the desired velocity was 0.1 mm/s and subjects were slower than the desired velocity when it was higher than 0.4 mm/s. For each admittance gain there is a different threshold velocity at which velocity-control accuracy is optimal in the aggregate. If the device operates at a velocity that is faster or slower than the threshold velocity the operator will tend to lag or lead the desired velocity, respectively.

# CONTENTS

<b>ABSTRACT</b> .....	<b>iii</b>
<b>LIST OF FIGURES</b> .....	<b>v</b>
<b>LIST OF TABLES</b> .....	<b>vii</b>
<b>ACKNOWLEDGEMENTS</b> .....	<b>viii</b>
<b>CHAPTERS</b>	
<b>1. INTRODUCTION</b> .....	<b>1</b>
<b>2. METHODS</b> .....	<b>7</b>
2.1 Hardware .....	7
2.2 Control System .....	8
2.3 Experimental Design .....	9
2.4 Evaluation Metrics .....	13
<b>3. RESULTS</b> .....	<b>16</b>
3.1 Scale .....	16
3.2 Accuracy .....	19
3.3 Precision .....	23
<b>4. DISCUSSION</b> .....	<b>27</b>
<b>5. CONCLUSION</b> .....	<b>36</b>
<b>REFERENCES</b> .....	<b>38</b>

## LIST OF FIGURES

1.1	Experimental setup, which consists of a 1-DOF admittance-type robotic device, a desktop computer, and a computer monitor. . . . .	4
2.1	Admittance-type robotic device used during the experiments. . . . .	7
2.2	Control system. . . . .	8
2.3	Screen shot of visual motion feedback that was provided to the test subject. . . . .	10
3.1	Raw data for metrics $E_d$ , $E_a$ , $C_v$ , and $RMS_n$ for different scale factors. These plots combine all $V_d$ values, all $k_a$ values, and all 10 subjects. . . . .	17
3.2	Experimental results for each metric $E_d$ , $E_a$ , $C_v$ , and $RMS_n$ for all subjects and trials for different levels of $S$ . The mean and 95% confident interval shown include all $k_a$ values used at each combination of $S$ and $V_d$ . . . . .	18
3.3	Raw data for metric $E_d$ for all ten subjects by admittance gain: (a) $k_a = 0.1$ , (b) $k_a = 0.4$ , (c) $k_a = 0.7$ , and (d) $k_a = 1.0$ . . . . .	20
3.4	Raw data for metric $E_a$ for all ten subjects by admittance gain: (a) $k_a = 0.1$ , (b) $k_a = 0.4$ , (c) $k_a = 0.7$ , and (d) $k_a = 1.0$ . . . . .	21
3.5	Experimental results for metric $E_d$ for all 10 subjects combined. $E_d$ is a measure of the subject's ability to maintain a constant desired velocity as a fraction of the desired velocity, as defined in (2.5). (a) shows $E_d$ across all $V_d$ values at different levels of $k_a$ , and (b) shows $E_d$ across all $k_a$ values at different levels of $V_d$ . . . . .	22
3.6	Experimental results for metric $E_a$ for all 10 subjects combined. $E_a$ is the absolute value of $E_d$ , which measures the subject's absolute error in tracking a desired velocity, as defined in (2.6). (a) shows $E_a$ across all $V_d$ values at different levels of $k_a$ , and (b) shows $E_a$ across all $k_a$ values at different levels of $V_d$ . . . . .	22
3.7	Raw data for metric $C_v$ for all ten subjects by admittance gain: (a) $k_a = 0.1$ , (b) $k_a = 0.4$ , (c) $k_a = 0.7$ , and (d) $k_a = 1.0$ . . . . .	24
3.8	Raw data for metric $RMS_n$ for all ten subjects by admittance gain: (a) $k_a = 0.1$ , (b) $k_a = 0.4$ , (c) $k_a = 0.7$ , and (d) $k_a = 1.0$ . . . . .	25
3.9	Experimental results for metric $C_v$ for all 10 subjects combined. $C_v$ is a measure of the subject's ability to maintain a constant velocity normalized by the subject's mean velocity, as defined in (2.7). (a) shows $C_v$ across all $V_d$ values at different levels of $k_a$ , and (b) shows $C_v$ across all $k_a$ values at different levels of $V_d$ . . . . .	26

3.10 Experimental results for metric  $RMS_n$  for all 10 subjects combined.  $RMS_n$  is a measure of the subject's velocity variation from the desired velocity, as defined in (2.8). (a) shows  $RMS_n$  across all  $V_d$  values at different levels of  $k_a$ , and (b) shows  $RMS_n$  across all  $k_a$  values at different levels of  $V_d$ . . . . . 26

4.1 Best force level in terms of accuracy for each admittance gain that was tested, as reported in Table 3.1. . . . . 30

4.2 Best force level in terms of accuracy for each desired velocity that was tested, as reported in Table 3.1. . . . . 30

4.3 Best admittance gain in terms of accuracy for each desired velocity that was tested, as reported in Table 3.1. . . . . 31

## LIST OF TABLES

2.1	Values used for the three variables tested during the experiments (desired velocity, admittance gain, scale). . . . .	11
2.2	Target force level determined according to (1.1) for each level of $V_d$ and $k_a$ used in the experiment. . . . .	12
2.3	Visual velocities that result from scaling the device velocity by $S$ , for scale values used in the experiment. . . . .	12
3.1	Desired velocities that result in optimal accuracy according to (2.5) for each admittance gain, determined by interpolating trends in Figure 3.5a. The force level is calculated for each admittance gain and velocity combination according to (1.1). . . . .	20
4.1	Variance in $E_d$ across all subject for each $V_d$ and $k_a$ combination. Variance was highest when $V_d$ was equal to 0.1 mm/s (highlighted in gray) . . . . .	31
4.2	Mean $E_a$ for each $V_d$ and $k_a$ combination, as shown in Figure 3.6. Values that are relatively high are highlighted in gray. . . . .	33
4.3	Target force levels (N) determined according to (1.1) for each level of $V_d$ (mm/s) and $k_a$ (mm/(N·s)) used in the experiment. Force levels highlighted in gray correspond to trials that had poor accuracy (high mean $E_a$ ), as seen in Table 4.2 and Figure 3.6. . . . .	34

## **ACKNOWLEDGEMENTS**

I would like to thank all those who helped make this research possible. I must first recognize the hand of God in all discovery and in my own life and successes. I also express my deepest gratitude to my dedicated, beautiful wife Sophia who supported and encouraged me as I conducted this research. I thank my wonderful parents, Alan and Karlynn Arbuckle, for selflessly supporting me in countless instances as I pursued my education. I am also grateful to my mother-in-law, Andrea Edwards, for her time and efforts. A special thanks to my professors Jake Abbott, Will Provancher, and Jon Butner, for offering me the wonderful opportunity to research under their guidance, and for teaching and directing me through the process. I also give thanks to Manikantan Nambi who has been a wonderful friend and mentor, to all my friends in the Telerobotics lab, and to all those who spent hours interacting with the admittance robot during my experiments.

# CHAPTER 1

## INTRODUCTION

Robots are commonly used to complete tasks that require a high degree of precision and accuracy. Fully autonomous robots are often designed to function within very tight tolerances and are used in precision tasks. However, autonomous robots generally require predefined operation procedures and are often limited to tasks that are either repetitive or performed in highly controlled environments. In contrast, robots that are controlled by a human operator can be used to perform tasks that are less predictable or where exact procedures cannot be predetermined. Using such a robot can augment a human's ability to complete a task that would otherwise be dangerous or impossible (e.g., in an environment that is toxic to humans). Robots can also be used to reduce or eliminate human error when high levels of accuracy or precision are required, such as in surgical tasks.

When a manipulation task requires a high degree of precision or accuracy, admittance-type robotic devices are often used. Admittance-type devices contain a great deal of gearing and inertia such that they appear nonbackdrivable to a human, and to many disturbances from the environment [1]. Admittance-type devices can be used to stably implement rigid systems, which is difficult to do using impedance-type devices (another common type of haptic robotic device that is backdrivable and has low inertia and low friction). An example of an existing robot that is used to reduce human error is the Johns Hopkins University Steady-Hand Robot [2–4], which operates on a precise scale not attainable by humans by effectively reducing the tremor in the human's hand. Another example of a robot that is used to improve human performance is the University of Utah Active Handrest [5–8], which is a handrest that moves intuitively to support the user's hand and enable fine motor control within a larger workspace than would otherwise be possible.

Admittance-type robots are controlled using admittance control; a human interacts directly with a force sensor mounted to the robot, and the robot is computer-controlled to move in response to the applied force. The most common and simplest type of admittance control is proportional-velocity control, where the admittance of the system reduces to a

simple gain,  $k$ , making the velocity of the robot,  $V$ , linearly proportional to the applied force  $F$ :

$$V = k_a F \quad (1.1)$$

If perfectly implemented, the control law (1.1) behaves like a massless viscous damper, with damping inversely proportional to  $k_a$  [9].

The admittance gain,  $k_a$ , can be tuned to adjust the user's experience when interacting with an admittance device. Implementing a low admittance gain in the control law (1.1) results in a sluggish or even fatiguing user experience because attaining desired velocities may require relatively high force input. On the other end of the spectrum, implementing a high admittance gain results in a very responsive system that can feel uncomfortable and even out of control; it feels as though the device is running away when the resultant velocity seems disproportionately high compared to the applied force. Nambi et al. [9] imply that humans feel most confident interacting with devices that are somewhat dissipative, and they suggest that there is a range of velocities and forces within which humans optimally interact with devices with their fingertip.

Since admittance-type devices move at a velocity that is proportional to the force that is applied on its sensor, the controllability of an admittance-type device is directly related to the operator's ability to control forces dexterously. Jones [10] reported that the coefficient of variation for both finger and elbow forces was significantly lower when both haptic and visual feedback were given (4%) than when just haptic feedback was given (12%). Srinivasan and Chen [11] conducted research on human ability to apply force on a static object. They found that humans have a mean absolute error of 11-15% of the target force value, when applying a constant force on a stationary target in the range of 0.25 N to 1.25 N with no visual feedback. Results from the same experiment showed that performance improved significantly and remained constant at 0.039 N (3-16% error) when visual force feedback was provided by rendering the target and applied forces on a computer monitor. In [11] the subjects were required to apply a constant force on a moving object, which required that they continuously detect the changes in force that occur as the device moved away, and simultaneously correct the position of the hand accordingly. Allin et al. [12] found that, when using the index finger, people have a just noticeable difference (JND) for force of 10% when the base force is 2.25 N and the subject is provided visual feedback. This force JND quantifies human ability to continuously detect a change in force application, and accounts for some of the variability that may be detected by the force sensor on the admittance-type device. Lederman et al. [13] also conducted a study on human force control on moving

objects. They studied the force variability in the normal direction as the subject moved their hand at different velocities (20 mm/s and 222 mm/s) in the tangential direction and under different force levels (user defined “low force” and “medium force”). They found that the end effector, force level, and velocity of the device all have a statistically significant effect on the mean force values. Hamilton et al. [14] reported that, while variability or noise is unavoidable during voluntary muscle contraction, the coefficient of variation of force is high for very low forces and decreases as force increases. [14, 15] predict that the decreased force variability results in part from the increase number of motor units activated in the muscle to attain higher forces.

Wu et al. [16] studied the effects of  $k_a$  and  $V$  on human force-control performance when interacting with an admittance device. The effect of velocity was studied independently of the admittance gain by running an admittance device with velocity control. Force measurements were recorded as test subjects attempted to apply a constant force on the device with their fingertip, which moved at a fixed velocity. A second test was also conducted where the device was controlled under admittance control. The velocity was not constant in the second test but was proportional to the applied force according to the control law (1.1). Wu et al. concluded that velocity, and not admittance gain, directly affects human force control. Nambi et al. [9] further investigated these results because they appeared to contradict anecdotal observations. Nambi et al. hypothesized that the results that Wu et al. reported were biased due to the nature of the experiment design. That is, data collected while the device operated under velocity control may not have been representative of performance under admittance-control. Also, in the experiments, the controller was turned on once the subject reached a desired force, which created large accelerations that may have affected the results of the tests. Additionally, the experiments were conducted without visual feedback, which required the subject to remember the desired force.

Nambi et al. conducted a similar experiment that was modified to eliminate concerns they had with the experiment conducted by Wu et al. Instead of comparing admittance control to velocity control, they compared human force precision under admittance control to human force precision in the isometric case (i.e., when the device does not move). Using an admittance device that is shown in Figure 1.1 (which is similar to the device used by Wu et al.) subjects’ force precision control was evaluated for a range of admittance gains and target forces. Subjects were given visual force feedback and asked to maintain a constant force on the device. The device either remained stationary or moved according to control law (1.1).

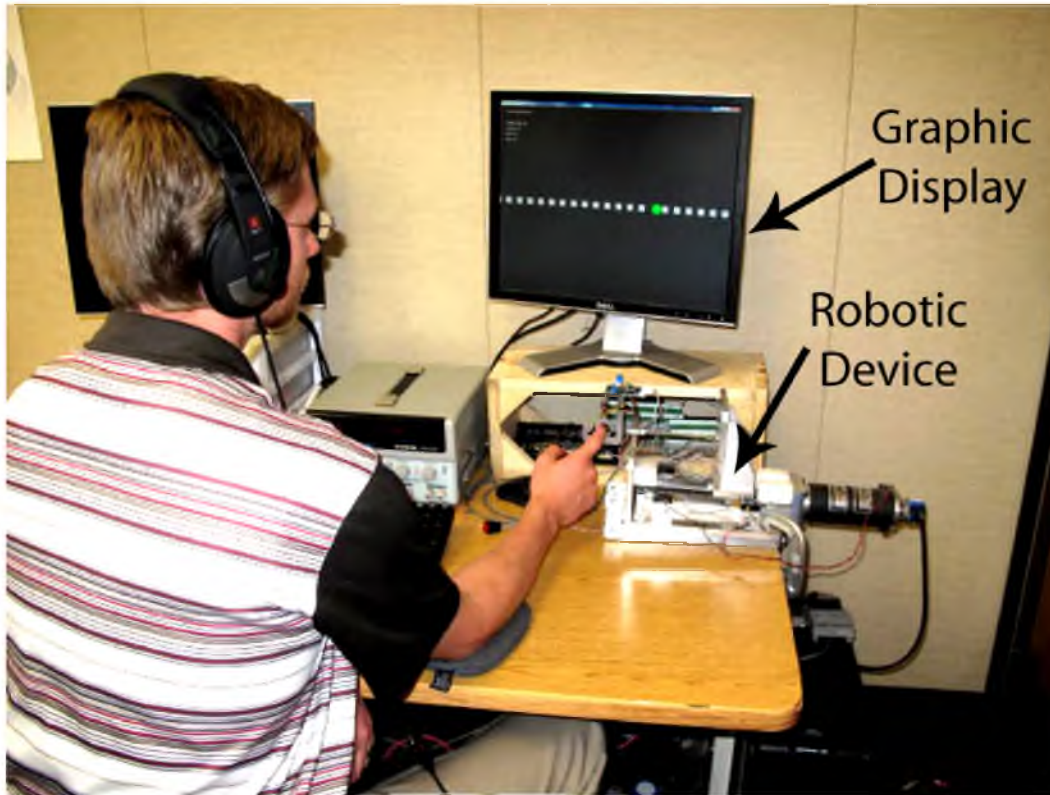


**Figure 1.1:** Experimental setup, which consists of a 1-DOF admittance-type robotic device, a desktop computer, and a computer monitor.

Nambi et al. reported that the nominal force was the most influential factor in determining a subject's ability to apply a precise constant force on an admittance-type device. They reported that force precision was poor for low nominal forces (under 0.5 N), which correlates with the observations of [14, 15] that muscle motor control decreases for decreased force levels. Furthermore, they found that, once force level had been accounted for, admittance gain was the second-most influential factor in determining force-control precision. They reported that when admittance gain was set to  $k_a = 0.1 \text{ mm}/(\text{N}\cdot\text{s})$  or less, force-control precision was found to be similar to the isometric case (i.e., when the device is stationary). Thus, there is a range of admittance gains for which optimal precision can be achieved.

Although this extremely low admittance gain does ensure high force-control precision, it does not result in an optimal user experience. Low admittance gains result in larger force requirements to attain a target velocity, which results in slow performance and user fatigue. To achieve the optimal user experience, it is necessary to understand the trade-off between force-control precision and user comfort. Furthermore, in real tasks the visual feedback will be the motion of the device and not an indicator of the force level as was shown in [9].

The goal of the experiment presented herein is to further quantify the performance characteristics of admittance control under different operating conditions. Whereas the previous experiment [9] was primarily concerned with subjects' ability to control their manually applied force on an admittance device, the study herein is primarily concerned with subjects' ability to control the velocity of the device. Since this study is focused on velocity control rather than force control, subjects were provided a visual target velocity and visual feedback of the device's motion, rather than the visual force feedback of [9] (the experimental setup used for the experiment reported herein is shown in Figure 1.1). This makes the present experiment more similar to actual manipulation tasks, since humans do not typically see force levels in real-world applications, rather, they see the device motion that results from applying a force on the device.

This study also explicitly considers the scaling factor that describes the relationship between the actual motion of the admittance device and the corresponding motion visually observed (e.g., on a monitor or in a microscope), since many applications that require a high degree of precision also require magnification of the workspace in order to provide useful visual feedback.

A common application that utilizes scaling between physical device motion and displayed motion is the implementation of a computer mouse. The cursor rendered on a computer monitor moves in its workspace with a velocity that is equal to the velocity of the mouse multiplied by a scale factor. Muñoz et al. [17] report that modifications of the scaling factor affect the task execution time and precision of positioning tasks. They studied human-computer interaction using the psychomotor model proposed by Fitts [18]. Fitts showed that the time required to complete a positioning task with an interface device depends on both the size of the target and the distance to the target. The study being reported in this thesis is not concerned with positioning tasks; however, we want to determine to what extent the scale factor affects human velocity control within the context of admittance control.

The experiment herein was conducted to determine under which operating conditions human velocity control is optimized for admittance devices that are controlled according to (1.1), and to determine the degradation in control under non-optimal conditions. Specifically, the experiment was conducted to determine the effects of admittance gain, velocity, and scale factor on human velocity control, given a visual and intuitive indication of a target velocity and visual feedback of the scaled motion of the device.

The outline of the remainder of this thesis is as follows: in Chapter 2 we describe the

design of our experiment; in Chapter 3 we include the results and analysis of our experiment; in Chapter 4 we provide additional discussion about the implications of the experimental results. We summarize our findings in Chapter 5.

## CHAPTER 2

### METHODS

#### 2.1 Hardware

The device used for this experiment was the same device that Nambi et al. [9] used during their experimentation. The device, shown in Figure 2.1, is a 1-DOF admittance-device that consists of a lead-screw-driven linear stage (Servo Systems Co. MLPS-4-10) driven by a DC motor (Servo Systems Co. 23MDC-LCSS). The DC motor has an optical encoder mounted to the motor shaft that is used to detect the motor position. The lead screw has a pitch of 12.7 mm and the encoder resolution is 4000 counts/rev after quadrature, which translates to a linear resolution of  $3\ \mu\text{m}$  for the linear stage. The force sensor has a sensitivity of 0.7 mN

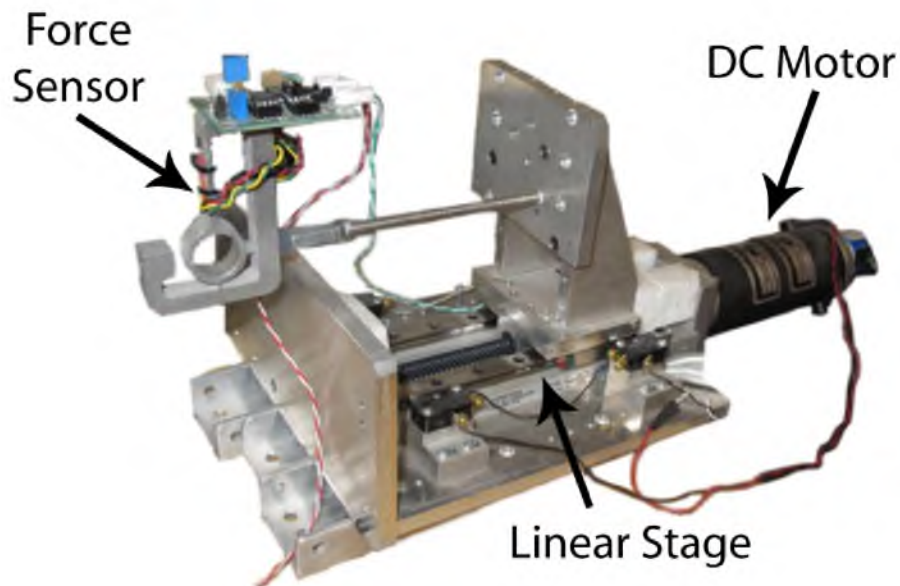


**Figure 2.1:** Admittance-type robotic device used during the experiments.

per bit (noise  $< 0.01$  N) and is mounted on the linear stage using a rigid rod. A Sensoray 626 DAQ card is used for data acquisition. It has a 16-bit ADC that is used to read force data and a 14-bit DAC, which is used to command voltage to the current amplifier (Advanced Motion Control 12 A8), powered by a 24-V linear power supply, which is used to power the DC motor. The voltage-to-current gain of the amplifier is 0.25 A/V. The software for the device was developed in C++ using the CHAI 3D library [19]. Visual feedback is provided to the subject on a 0.5 m computer screen placed at a distance of 1.5 m from the user. The force readings are sampled at 1 kHz and graphics are displayed at 60 Hz.

## 2.2 Control System

The PD-plus-feedforward controller that was implemented in the device is shown in Figure 2.2. Unit-DC-gain digital low-pass filters  $G_1$  and  $G_2$  with time constants  $\tau_1 = 0.001$  s and  $\tau_2 = 0.0005$  s were used to reduce quantization error and differentiation noise. The proportional gain  $K_p$  was set at 30 V/mm and derivative gain  $K_d$  was set at 0.1 (V·s)/mm for the majority of the experiments. The proportional gain  $K_p$  was increased to 60 V/mm for low velocities of 0.1 mm/s and 0.2 mm/s to improve tracking. Nambi et al. empirically found these gain values give the minimal tracking error for sinusoidal position trajectories (more detail can be found in [9]). The controller gains automatically adjusted according to the target velocity in each trial, and were held constant for a given trial. The feedforward model for the device was experimentally derived and is given by the voltage  $E_{ff} = 0.06V_c +$

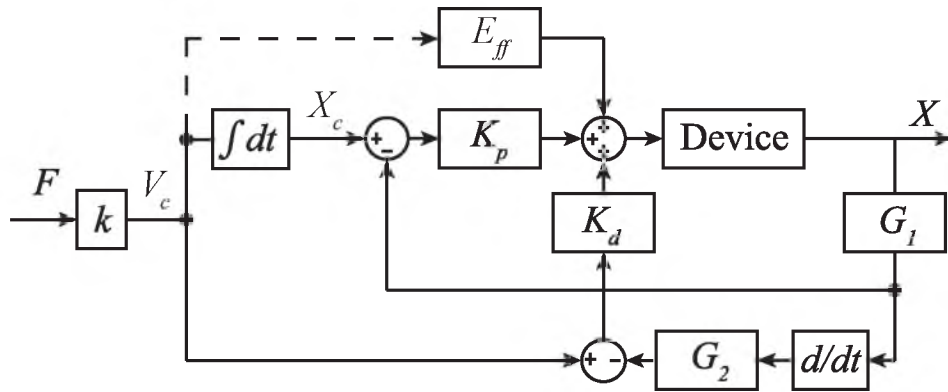


Figure 2.2: Control system.

$2.2(1 - e^{(-3.3V_c)})$  V·s/mm, where  $V$  is the commanded velocity. This feedforward model is a smooth function that approximates Coulomb-plus-viscous friction. The inputs for the system are calculated as:

$$V_c(n) = kF(n) \quad (2.1)$$

$$X_c(n+1) = X_c(n) + V_c(n)\Delta t \quad (2.2)$$

$F(n)$  is the force applied by the user at sample  $n$ .  $X_c(n)$  is the commanded position of the device at sample  $n$ , which is found by numerically integrating the desired velocity.  $\Delta t$  is the sampling time of the control system (1 ms). Nambi et al. found that the controlled device is capable of tracking signals at frequencies below 7 Hz (44 rad/s), for the amplifier of interest, which is sufficient for signals of interest herein.

## 2.3 Experimental Design

Our goal was to determine the effect that visual position/velocity feedback has on human velocity control of an admittance-type device. Experiments done in prior work provided the subject with visual force feedback using a graphical display that showed both the applied force and the target force. In real-world applications humans do not visually perceive force, but rather the motion that results from applying a force on a body. We were interested in determining how visual motion feedback affects human ability to precisely command a velocity on an admittance-device, and how the admittance gain  $k_a$ , the desired velocity  $V_d$ , and the scale factor,  $S$ , interact with visual velocity feedback.

The experiment, which had institutional review board approval (Ref Number 7514886), was performed by 10 right-handed subjects using their right index fingers. Figure 2.3 shows a screen capture of the visual feedback that was shown to the user. The visual target velocity was displayed as a continuous stream of white squares that move across the computer monitor from right to left at a constant velocity, which was predetermined for each trial. A colored sphere, rendered over the stream of squares, represented the position of the admittance device end-effector multiplied by a scale factor. As the subject moved the end-effector, the colored sphere moved accordingly, giving an accurate indication of the velocity of the admittance device. This scenario is relevant to real world applications where the admittance-device is operated on a scale that cannot easily be detected by the human eye. Such applications would inherently require high precision since humans are not capable of functioning precisely on such scales. The effect of scaling the visual velocity feedback was also considered in this experiment to determine if human performance is affected by a difference between physical velocity and visual velocity. The scale factors that were

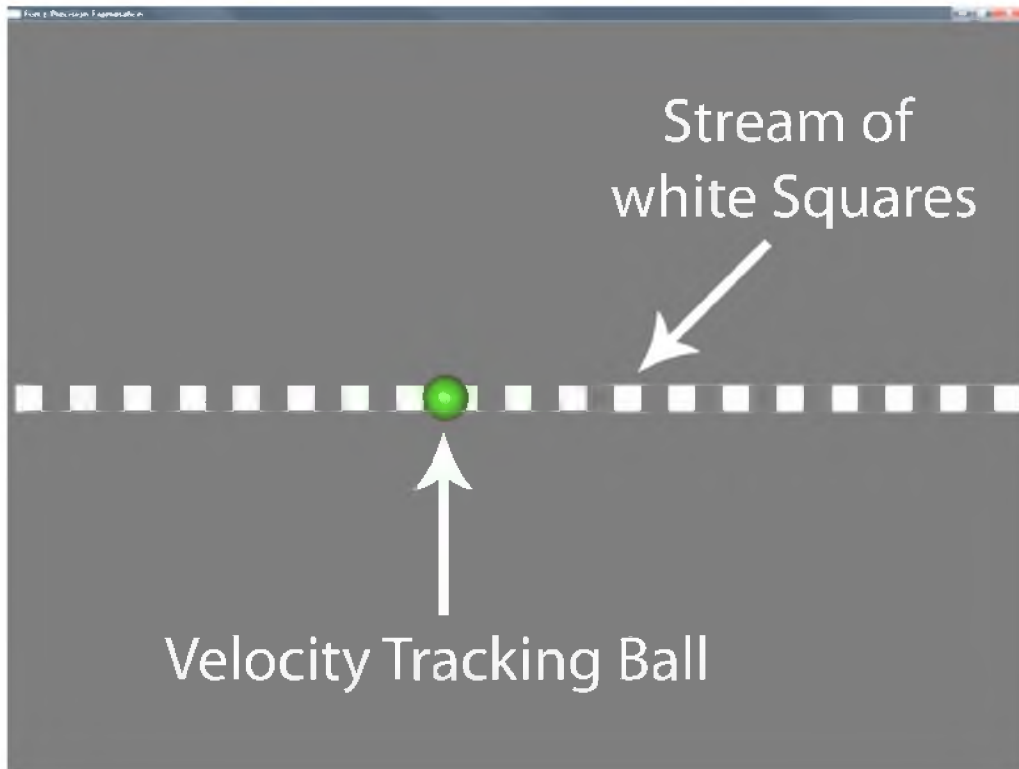


**Figure 2.3:** Screen shot of visual motion feedback that was provided to the test subject.

implemented during the trial are 30, 45, 60, and 75, meaning that if the admittance device was commanded to move at a rate of 1 mm/s, the colored sphere would move across the display at 30, 45, 60, or 75 mm/s, respectively. The scale factors were selected such that the motion of the sphere was perceivable for the slowest velocities and did not move off the computer screen for the fastest velocities, during a 4.5 second trial.

The best size and shape for the graphics that were streamed across the visual display were determined by trial and error. Initially, the graphics stream was made up of thin, vertical, white lines that were close together. This configuration proved to be uncomfortable to look at and distorted velocity perception for some velocities. The discomfort and distortion was reduced when using thicker, shorter lines. Ultimately, a square was used because the sphere stood out more when the stream objects were smaller than the sphere. It was observed in pilot studies that when the spacing between the squares was made large enough that the sphere could fit between 2 squares, then the subjects would often attempt to do just that. This added an undesirable positioning component to the experiment (e.g., even if the sphere and squares were already moving across the screen at the same velocity, the user would make an adjustment to get the sphere in between two squares). By making

the spacing between the squares slightly smaller than the sphere diameter, this problem was eliminated. Another problem occurred during trials that implemented slow velocities: the width of the squares would grow and shrink as the squares slowly moved from one pixel to the next. The stream appeared to inch-worm across the display because the pixels on the leading edge of the square and those on the trailing edge did not turn on and off synchronously. OpenGL has a method that implements anti-aliasing of the graphics but it did not solve this problem. In addition to using anti-aliasing, the width of the squares was manually set equal to the width of 10 pixels. Implementing these two changes together ensures that the trailing edge of the squares fade on and off together.

During the experiment the subjects were asked to match the velocity of the colored sphere to the velocity of the stream of white squares by applying a force on the force sensor. Subjects rested their elbow on the table and applied a force to the left, which was also the direction of motion for both the device and the visual target velocity. Each trial began when the subject applied a force on the sensor that was 20% higher than the sensor noise (noise < 0.01 N). The force required to trigger the device was so low that it did not affect the user’s ability to control the device (i.e., there was no sense of sticking at the beginning of a trial).

Each trial tested the subject’s performance for different combinations of  $k_a$ ,  $V_d$ , and  $S$ . The values that were used during the experiments are shown in Table 2.1. Every combination of  $k_a$ ,  $V_d$ , and  $S$  was tested, resulting in 64 trials per test. The 64 trials were administered randomly to ensure that ordering had no effect on the results of the testing. Subjects repeated each set of 64 trials four times, sequentially, with a different random ordering each time, making a total of 256 trials in the complete experiment.

The range of admittance gains and velocities used in this experiment were selected based on the results that Nambi et al. reported. The force values are determined by (1.1) and thus are proportional to  $V_d$  and  $k_a$ . The range of  $V_d$  and  $k_a$  for this experiment were selected to be between 0.1 and 1.0, resulting in force values between 0.1 N and 10.0 N, as shown in Table

**Table 2.1:** Values used for the three variables tested during the experiments (desired velocity, admittance gain, scale).

$V_d$ (mm/s)	$k_a$ (mm/(N·s))	$S$
0.1	0.1	30
0.4	0.4	45
0.7	0.7	60
1.0	1.0	75

2.2. Velocities that were displayed on the visual display were determined by multiplying the desired velocity by the scale factor and are shown in Table 2.3.

Each trial lasted 4.5 seconds, but only the last two seconds of each trial was considered in the data analysis. The first 2.5 seconds were eliminated to account for the ramp-up time required for a subject to attain a specified velocity. Pilot testing showed that two seconds was enough ramp-up time to achieve 90% of the force required to attain all desired velocities. The experiment lasted between 45 minutes and 1 hour for each subject. White noise was played through headphones during the experiment to eliminate audio feedback of the device movement and other distractions. Subjects were allowed to rest at any time during the experiment, but this was rarely necessary. In the event that a subject's performance was poor due to any outside influences, subjects were permitted to re-attempt trials. Before the experiment began, subjects were required to interact with the device for about five minutes. During this practice time subjects were allowed to manually set the  $k_a$ ,  $V_d$ , and  $S$  values to levels that are within the range of values being tested herein. They became familiar with interacting with the device under the full spectrum of operating conditions to mitigate the effect of randomly varying the operating conditions between trials.

A pilot test was conducted to ensure that enough data was collected from each subject. Two test subjects were administered the test eight times sequentially, making a total of 512 trials each. These data were used to determine the statistical reliability,  $R$ , of the metrics being used (the metrics are described in the next section). The reliability was calculated for

**Table 2.2:** Target force level determined according to (1.1) for each level of  $V_d$  and  $k_a$  used in the experiment.

$V_d \backslash k_a$	0.1	0.4	0.7	1.0
0.1	1.0	0.25	0.14	0.1
0.4	4.0	1.0	0.57	0.4
0.7	7.0	1.75	1.0	0.7
1.0	10.0	2.5	1.43	1.0

**Table 2.3:** Visual velocities that result from scaling the device velocity by  $S$ , for scale values used in the experiment.

$V_d \backslash S$	30	45	60	75
0.1	3.0	4.5	6.0	7.5
0.4	12.0	18.0	24.0	30.0
0.7	21.0	31.5	42.0	52.5
1.0	30.0	45.0	60.0	75.0

each subject independently. Reliability shows how consistent the metrics are in measuring a phenomenon. The statistical model of a metric with low reliability will have a large amount of variation that is not accounted for by its predictors. This excess variation is considered error in the model and is used to quantify the reliability of the metrics. To calculate the reliability a fixed-factor univariate ANOVA model of the metrics was conducted with  $V_d$ ,  $k_a$ , and  $S$  as factors. Reliability was calculated using the sum of squares of the model,  $m$ , and sum of squares of the error,  $e$ , in the model.

$$R = \frac{m}{m + e} \quad (2.3)$$

The reliabilities were determined to be greater than 90% for all of the metrics in question; however, we were not necessarily concerned with the actual level of reliability. Rather, we were interested in knowing how the reliability was affected when the number of trials was reduced. Using the Spearman-Brown prediction equation (2.4) the reliability of each metric could be predicted for tests that consisted of only 256 trials (which would cut the experimentation time in half). (2.4) determines an adjusted reliability,  $R^*$ , for each metric given the percentage,  $N$ , by which the number of trials was reduced:

$$R^* = \frac{N \cdot R}{1 + (N - 1) R} \quad (2.4)$$

By reducing the number of trials from 512 to 256 ( $N = 0.5$ ) the prediction showed a reduction in reliability of less than 5%. This slight reduction was deemed permissible given that the initial reliability was relatively high to begin with.

After initial analysis of the trials, additional metrics were included in the study to gain a better understanding of human velocity-control accuracy (see the next section for more information about the accuracy metrics). These metrics were not as reliable as the previous precision metrics and would have benefited from a larger sample size. This means that the models of the accuracy metrics had a large amount of variation in them that was not accounted for by the predictors ( $V_d$ ,  $k_a$ , and  $S$ ). This variation is due to factors that were not studied in this experiment, such as the subject's mental state, or physical aptitude for this type of test, or even the variability inherent in human motor control. Since we are only interested in understanding the effects of the desired velocity, admittance gain, and scale, all other factors were generalized as human variability.

## 2.4 Evaluation Metrics

In order to understand human velocity control of a haptic device controlled under admittance-control, performance was considered in terms of precision and accuracy. In this

experiment, accuracy was determined by a subject's ability to track the desired velocity, and was calculated independent of the velocity variation about the subject's mean velocity. Quantitatively, accuracy was determined by the difference between the mean velocity and the desired velocity for each trial. This difference is a measure of the velocity error from the desired velocity. Dividing the velocity error by the desired velocity normalized the error:

$$E_d = \frac{\bar{V} - V_d}{V_d} \quad (2.5)$$

where  $\bar{V}$  is the mean velocity of the device and  $V_d$  is the desired velocity for each trial.

The absolute normalized error from the desired velocity, given by (2.6), shows the magnitude of the error irrespective of whether the velocity was faster or slower than the desired velocity:

$$E_a = \left| \frac{\bar{V} - V_d}{V_d} \right| \quad (2.6)$$

$E_a$  is more effective than  $E_d$  at showing the accuracy for the whole data set because it is an absolute metric.

In this experiment, high precision was achieved when the variation in the device's velocity about the mean velocity was minimal. The coefficient of variation of velocity,  $C_v$ , quantified precision in terms of the standard deviation of velocity normalized by the mean velocity:

$$C_v = \frac{\sigma}{\mu} \quad (2.7)$$

where  $\sigma$  is the standard deviation of the velocity and  $\mu$  is the mean velocity for each trial. In addition to evaluating  $C_v$ , the *RMS* of the velocity was considered to measure precision. Normalizing the *RMS* by the desired velocity makes this metric comparable to  $C_v$ :

$$RMS_n = \frac{1}{V_d} \sqrt{\frac{\sum_i (V_i - V_d)^2}{N}} \quad (2.8)$$

$C_v$  and  $RMS_n$  are only slightly different:  $RMS_n$  quantifies precision in terms of the desired velocity,  $V_d$ , whereas  $C_v$  is in terms of the actual mean velocity,  $\mu$ . Expanding  $C_v$  makes this fact clear:

$$C_v = \frac{\sigma}{\mu} = \frac{1}{\mu} \sqrt{VAR(V)} = \frac{1}{\mu} \sqrt{\frac{\sum_i (V_i - \mu)^2}{N}} \quad (2.9)$$

Precision, quantified in terms of the average velocity,  $\mu$ , accounts for the subject's ability to maintain a constant velocity, independent of what velocity is being held constant.  $RMS_n$  shows how precisely the subject can maintain the desired velocity. Both metrics can be thought of as quantifying tremor, though  $RMS_n$  is influenced by the desired velocity, which may not be necessary to consider when quantifying precision.

Both Nambi et al. [9] and Jones [10] use a metric that is similar to the metric  $C_v$  (coefficient of variation of velocity) to measure tremor. Similar to this thesis, [10] uses the coefficient of variation to quantify tremor; however, it is formulated in terms of force instead of velocity. [9] also quantified tremor, but they used the normalized mean absolute deviation ( $MAD_t$ ) to quantify the tremor in terms of deviation from the mean applied force. All three metrics were used to understand how consistently a subject applied a constant force for a period of time. This information give insight into how precisely humans can control force (or velocity in the case of this thesis) while interacting with an admittance-type haptic device. [9] reported the normalized force error ( $E_t$ ), which is very similar to the metric  $E_d$  used in this thesis.  $E_d$  was used herein to quantify human velocity control accuracy, while [9] used  $E_t$  to compare human force-control error, while interacting with an admittance-type device, to the force-control error present in the static case. [10] also measured the error in human force control; however, Jones used the mean absolute error of the force, which is similar to the metric  $E_a$  (absolute normalized error of velocity), except  $E_a$  is in terms of velocity and not force, and [10] did not normalize the error. Both  $E_d$  and  $E_a$  are used in this thesis to quantify human velocity-control accuracy, or the ability to track a desired velocity over time.

## CHAPTER 3

### RESULTS

We are interested in understanding the effect that each variable (scaling factor, desired velocity, and admittance gain) had on the accuracy and precision of human velocity control. In Section 3.1 we show that scale does not effect human velocity-control precision and has a very limited effect on accuracy. Furthermore, in the limited situations where  $S$  is shown to have an effect,  $V_d$  and  $k_a$  have an effect that is much greater than that of  $S$ . Therefore, for all subsequent sections  $S$  is not considered in the statistical analyses, and the data collected under the four different scaling values will simply act to increase the total number of data points gathered at each of the combinations of  $k_a$  and  $V_d$ .

#### 3.1 Scale

Figure 3.1 shows the raw data for the metrics  $E_d$ ,  $E_a$ ,  $C_v$ , and  $RMS_n$  for different scale factors. These plots combine all  $V_d$  values, all  $k_a$  values, and all 10 subjects. The raw data give a good sense of the magnitude of the variation that is occurring in each metric.

Figure 3.2 shows the experimental results for each metric  $E_d$ ,  $E_a$ ,  $C_v$ , and  $RMS_n$  for all subjects and trials for different levels of  $S$  at different  $V_d$ . Figure 3.2 explores the role of  $S$  on the four metrics for the complete experimental data set. The general lack of variation in  $E_d$ ,  $E_a$ ,  $C_v$ , and  $RMS_n$  across values of  $S$  seems to indicate that velocity control performance is not dependent on scaling, at least for the range of scaling values considered here. There is, however, one exception to this observation;  $E_a$  does seem to have some variation when  $V_d$  is equal to 0.1 mm/s. To test this and all the models described in this study we used a mixed-effects ANOVA model with a Maximum Likelihood estimator in SPSS 19 (SPSS Mixed), which parallels a mixed-factor ANOVA. This allows us to simultaneously account for effects within trials, within subjects, and between trials and subjects for proper estimation. The key differences between this method and a standard ANOVA model are due to the estimation procedure that allows for more complex model testing by implementing an asymptotically correct estimation procedure (rather than the finite sample assumptions

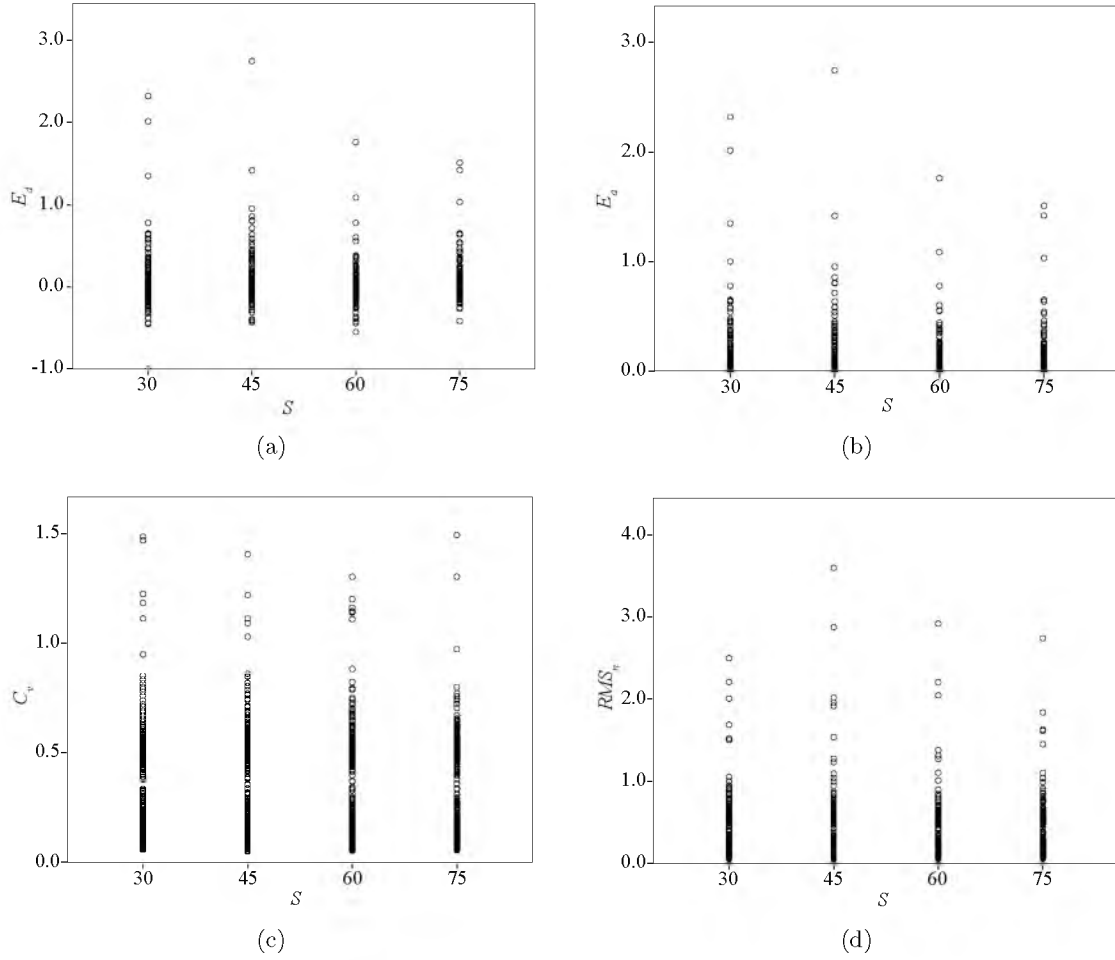


**Figure 3.1:** Raw data for metrics  $E_d$ ,  $E_a$ ,  $C_v$ , and  $RMS_n$  for different scale factors. These plots combine all  $V_d$  values, all  $k_a$  values, and all 10 subjects.

of the standard mixed-factor ANOVA). For ease of use, all results are reported akin to a mixed-factor ANOVA and all independent variables were treated as categories. In every case, conventional significance was determined at  $\alpha = 0.05$ , two tailed.

The effect of  $S$  was not significant,  $F(3, 2487) = 1.262$ ,  $p = 0.286$ , in a model of  $E_d$  that included  $S$ ,  $k_a$ , and  $V_d$  and their interactions. The effect of  $S$  was not significant,  $F(3, 2486) = 0.373$ ,  $p = 0.773$ , in a model of  $C_v$  that included  $S$ ,  $k_a$ , and  $V_d$ , and their interactions. The effect of  $S$  was not significant,  $F(3, 2487) = 0.864$ ,  $p = 0.459$ , in a model of  $RMS_n$  that included  $S$ ,  $k_a$ , and  $V_d$ , and their interactions. However, the effect of  $S$  was significant,  $F(3, 2487) = 3.165$ ,  $p = 0.024$ , in a model of  $E_a$  that included  $S$ ,  $k_a$ , and  $V_d$ , and their interactions; the  $V_d$ -by- $S$  interaction was also significant,  $F(9, 2487) = 2.358$ ,  $p = 0.012$ .

The scale factor,  $S$ , was only significant for the metric  $E_a$ , which is an absolute measure of accuracy. Close inspection of Figure 3.2b shows that the variation in  $E_a$  only seems

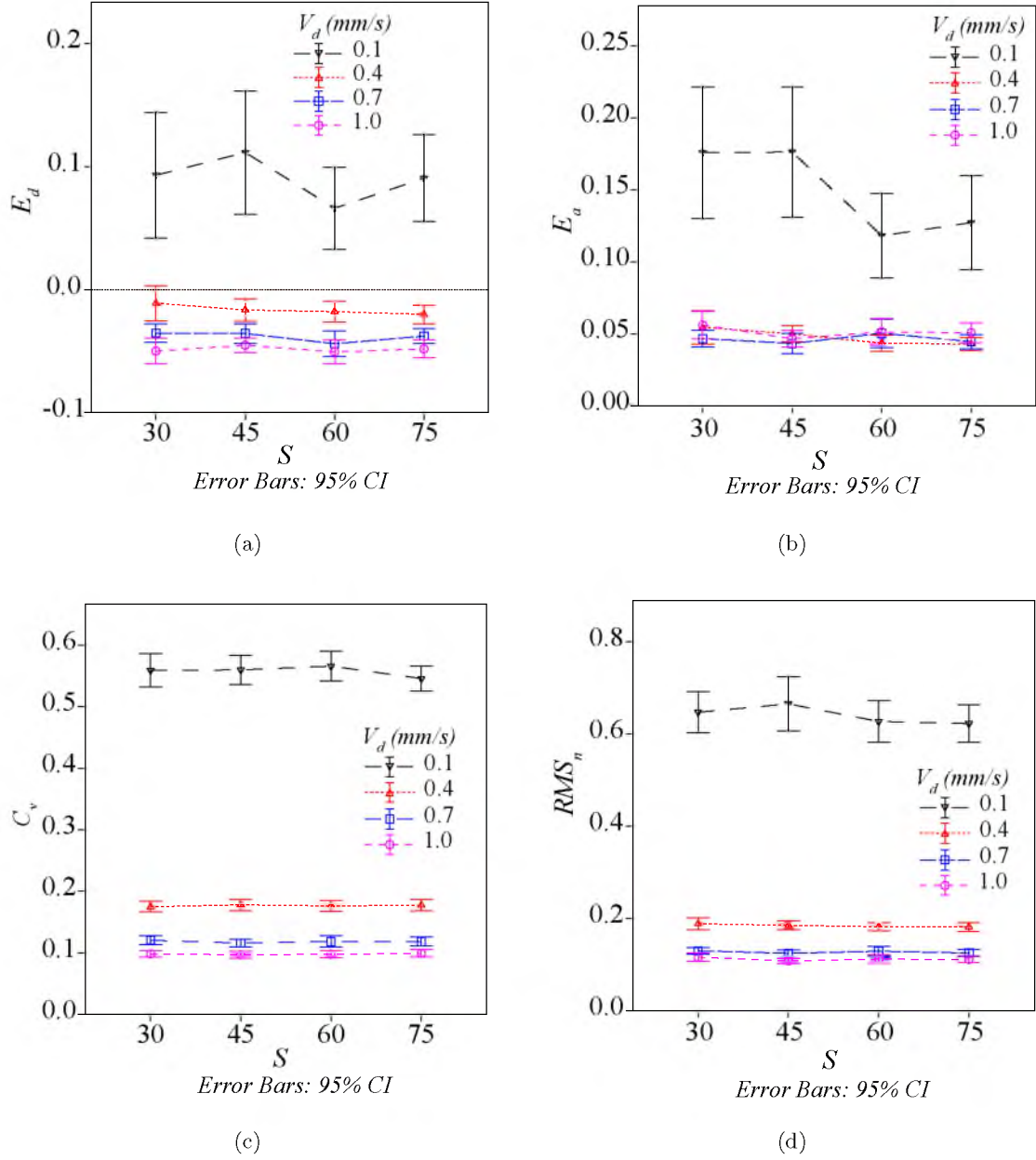


**Figure 3.2:** Experimental results for each metric  $E_d$ ,  $E_a$ ,  $C_v$ , and  $RMS_n$  for all subjects and trials for different levels of  $S$ . The mean and 95% confident interval shown include all  $k_a$  values used at each combination of  $S$  and  $V_d$ .

to occur when  $V_d$  was equal to 0.1 mm/s. Further statistical analysis shows that  $S$  was significant,  $F(3,2541) = 2.611$ ,  $p = 0.050$ , when  $V_d$  was equal to 0.1 mm/s in a model of  $E_a$  that included  $S$ ,  $k_a$ , four categorical divisions of  $V_d$ , and all  $V_d$ -by- $S$  interactions. The same model configuration of  $E_a$  showed that  $S$  was not significant for all other levels of  $V_d$ :  $F(3,2541) = 0.291$ ,  $p = 0.832$  when  $V_d$  equals 0.4 mm/s,  $F(3,2541) = 0.090$ ,  $p = 0.966$  when  $V_d$  equals 0.7 mm/s, and  $F(3,2541) = 0.141$ ,  $p = 0.936$  when  $V_d$  equals 1.0 mm/s.

These statistical evaluations show that  $S$  affects  $E_a$  only when  $V_d$  is equal to 0.1 mm/s, and otherwise has no effect on any metric. Figure 3.2b shows that there is a slight improvement in performance when the scale factor is increased from 45 to 60. These scale factors correlate with visual velocities of 4.5 mm/s and 6 mm/s, which are rendered on a computer monitor (the desired velocity ( $V_d$ ) of the device remains 0.1 mm/s). Therefore, it appears that human velocity-control accuracy ( $E_a$ ) degrades when the visual velocity is 4.5 mm/s or slower. By increasing the scale factor from 45 to 60 there is an improvement of just over 12% for a  $V_d$  of 0.1 mm/s, while increasing  $V_d$  and maintaining  $S$  the same improves accuracy by almost 30%. This shows that for the range of velocities we are considering,  $S$  has very little effect when compared to the effects of  $V_d$  and  $k_a$ , as can be seen in Figure 3.2b (this will be discussed in more depth in Section 3.2). It is important to note that the scale factor does not have any further influence on velocity tracking performance, at least for the range of scales and velocities considered in this experiment. Therefore, for the remainder of this paper  $S$  will not be considered in the statistical analyses.

### 3.2 Accuracy

The raw data for both  $E_d$  and  $E_a$  are shown in Figure 3.3 and Figure 3.4, respectively. The raw data are shown to give a true sense of the range of the variation seen in each metric between subjects and trials. The raw data show the magnitude of the deviation from the means that are shown in Figure 3.5 and Figure 3.6.

The metric  $E_d$  is a measure of how accurately a subject could track a desired velocity. The effect of  $V_d$  was significant,  $F(3,2535) = 127.503$ ,  $p < 0.001$ , as was the effect of  $k_a$ ,  $F(3,2535) = 21.683$ ,  $p < 0.001$ , in a model of  $E_d$  that included  $k_a$ ,  $V_d$ , and the  $k_a$ -by- $V_d$  interaction; the interaction was also significant,  $F(9,2535) = 8.035$ ,  $p < 0.001$ . Figure 3.5a shows the relationship between  $E_d$  and  $V_d$  for all  $k_a$  used in the experiment. Since  $E_d$  is normalized by  $V_d$ , data from all trials can be compared directly, regardless of velocity levels. An  $E_d$  value of zero indicates perfect performance, or in this case, perfect accuracy. However,  $E_d$  is not in terms of absolute error and does not give a complete sense of accuracy for the whole body of trials. Rather,  $E_d$  shows whether the subjects tended to move faster or slower than the desired velocity. Figure 3.5a shows that on average subjects moved faster than the desired velocity when the desired velocity was 0.1 mm/s and subjects were slower than the desired velocity when it was higher than 0.4 mm/s. This trend suggests that there is an optimal configuration where, on average, test subjects will move at the desired velocity. Theoretically, the optimal velocity corresponds to an  $E_d$  of zero for each

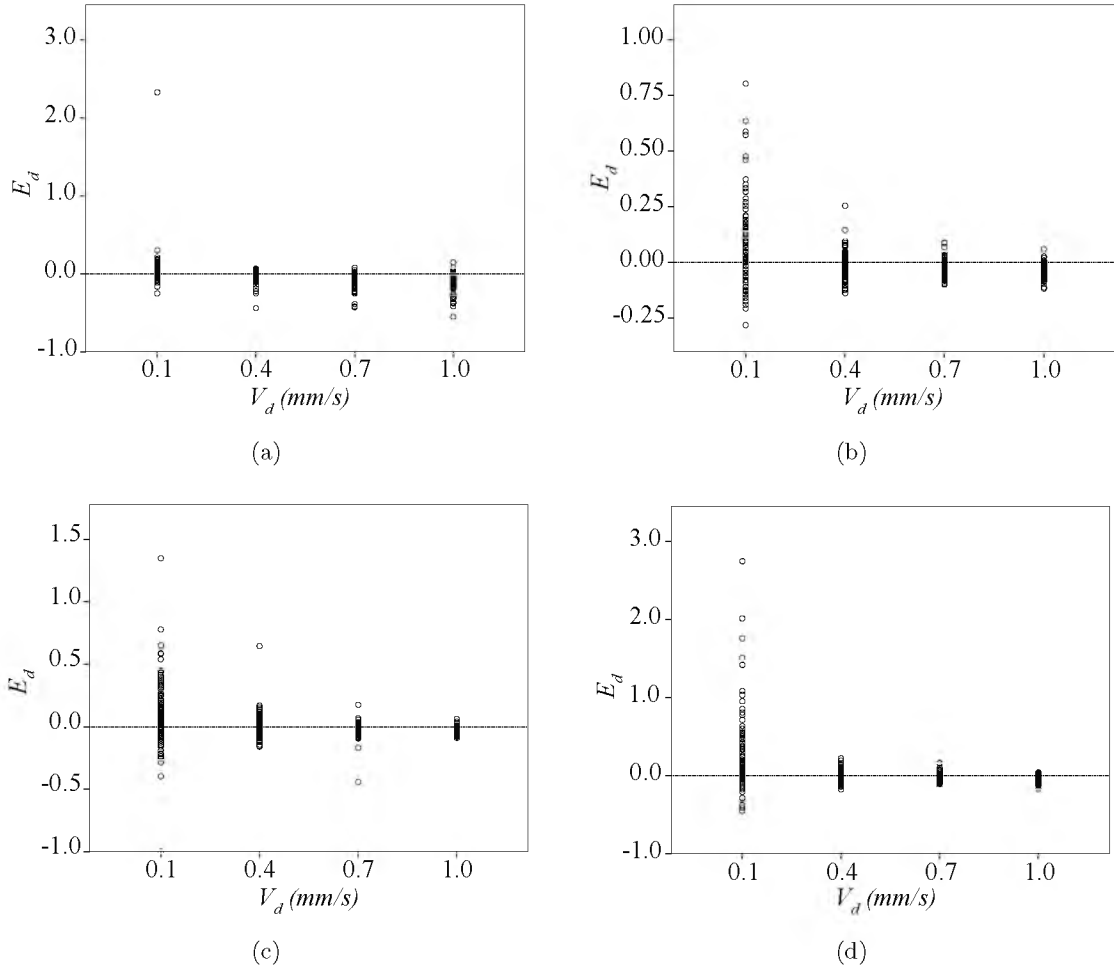


**Figure 3.3:** Raw data for metric  $E_d$  for all ten subjects by admittance gain: (a)  $k_a = 0.1$ , (b)  $k_a = 0.4$ , (c)  $k_a = 0.7$ , and (d)  $k_a = 1.0$ .

**Table 3.1:** Desired velocities that result in optimal accuracy according to (2.5) for each admittance gain, determined by interpolating trends in Figure 3.5a. The force level is calculated for each admittance gain and velocity combination according to (1.1).

$k_a$ (mm/(N·s))	$V_d$ (mm/s)	$F$ (N)
0.1	0.27	2.7
0.4	0.32	0.8
0.7	0.37	0.53
1.0	0.4	0.4

admittance gain. A linear interpolation of the trends in Figure 3.5a gives a rough estimate of the theoretical optimal velocities for each admittance gain, as shown in Table 3.1. Figure 3.5b shows that, for a given admittance gain, a velocity of 0.4 mm/s will result in the least amount of inaccuracies and the device velocity will generally be slower than or equal to the

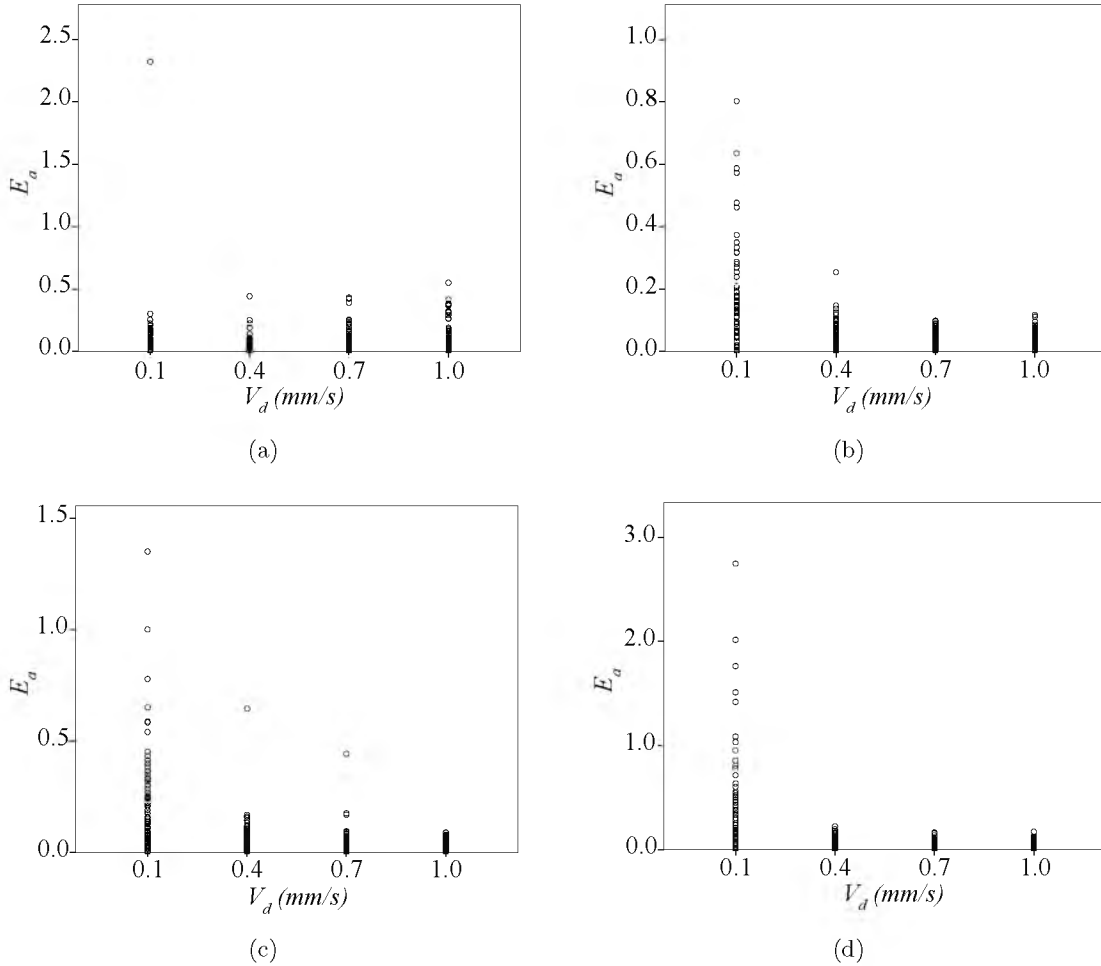


**Figure 3.4:** Raw data for metric  $E_a$  for all ten subjects by admittance gain: (a)  $k_a = 0.1$ , (b)  $k_a = 0.4$ , (c)  $k_a = 0.7$ , and (d)  $k_a = 1.0$ .

desired velocity. Figure 3.5b shows that for some velocities the subjects' average accuracy was never optimal, which suggests that for some velocities subjects will always tend to lead or lag the desired velocity, regardless of the admittance relationship between force and velocity. Therefore, it is simpler to select an admittance gain and then determine the best desired velocity, rather than choosing the desired velocity first and then finding the corresponding best admittance gain. This is fortuitous, considering that the admittance gain is often a quasistatic parameter in admittance-type systems, and the desired velocity is chosen in real time by the human user.

$E_a$  is the absolute value of  $E_d$  and shows the velocity error in terms of the magnitude of the error. The effect of  $V_d$  was significant,  $F(3,2535) = 101.87$ ,  $p < 0.001$ , as was the effect of  $k_a$ ,  $F(3,2535) = 11.143$ ,  $p < 0.001$ , in a model of  $E_a$  that included  $k_a$ ,  $V_d$ , and the  $k_a$ -by- $V_d$  interaction; the interaction was also significant,  $F(9,2535) = 17.024$ ,  $p < 0.001$ . Figure 3.6a

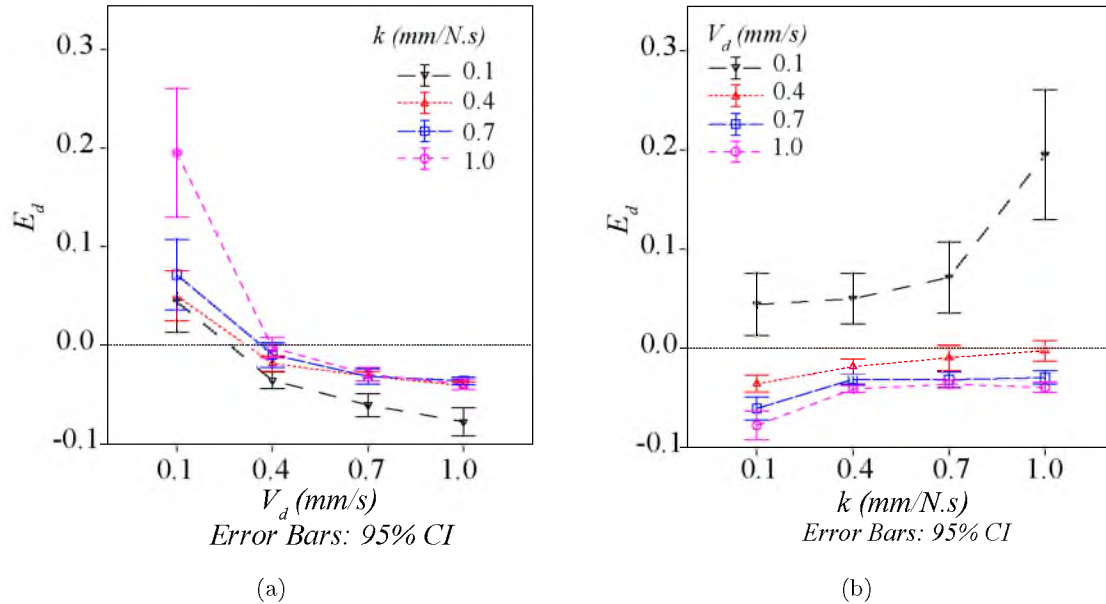


**Figure 3.5:** Experimental results for metric  $E_d$  for all 10 subjects combined.  $E_d$  is a measure of the subject's ability to maintain a constant desired velocity as a fraction of the desired velocity, as defined in (2.5). (a) shows  $E_d$  across all  $V_d$  values at different levels of  $k_a$ , and (b) shows  $E_d$  across all  $k_a$  values at different levels of  $V_d$ .

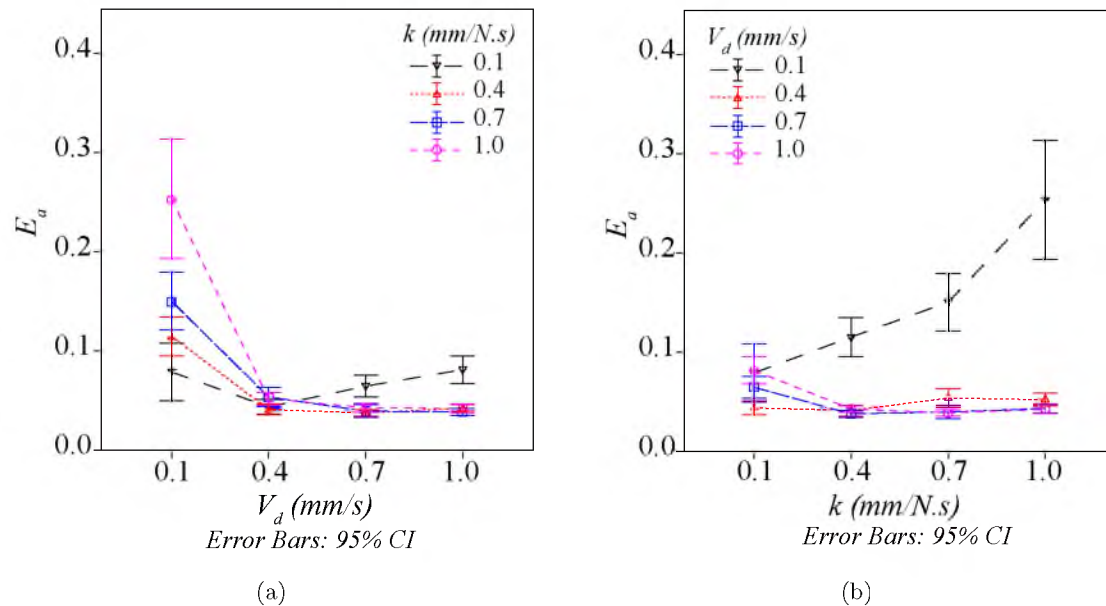


**Figure 3.6:** Experimental results for metric  $E_a$  for all 10 subjects combined.  $E_a$  is the absolute value of  $E_d$ , which measures the subject's absolute error in tracking a desired velocity, as defined in (2.6). (a) shows  $E_a$  across all  $V_d$  values at different levels of  $k_a$ , and (b) shows  $E_a$  across all  $k_a$  values at different levels of  $V_d$ .

shows the relationship between  $E_a$  and  $V_d$  for each value of  $k_a$ . Since  $E_a$  represents the absolute value of velocity error the optimal  $V_d$  corresponds to the lowest value of  $E_a$ . Since there are no combinations of admittance gain and desired velocity that result in an  $E_a$  of zero it shows that, on average, perfect accuracy was not achieved by the subjects, which is expected. Figure 3.6a makes it clear that accuracy is poor for trials conducted with a desired velocity of 0.1 mm/s. This observation is validated by Figure 3.3, which shows significantly more variation in the data for a  $V_d$  of 0.1 mm/s than for other values (although some of the variation is explained by the effect of scale seen in Figure 3.2b). When  $V_d$  is equal to 0.1 mm/s, performance results are best when  $k_a$  is set to 0.1 mm/N·s. In contrast, when  $V_d$  is larger than 0.4 mm/s, a  $k_a$  value of 0.1 mm/N·s results in the poorest performance. When  $V_d$  is exactly 0.4 mm/s, all  $k_a$  values result in nearly the same performance. It is apparent that performance is poor when either  $k_a$  or  $V_d$  are set to a value of 0.1, and that the best performance occurs during trials that are conducted with  $k_a$  and  $V_d$  values that are greater than 0.1. The only exception is when  $k_a$  is equal to 0.1 mm/N·s and  $V_d$  is equal to 0.4 mm/s. It appears that performance may suffer when applied force is too low (high  $k_a$ , low  $V_d$ ) or too high (low  $k_a$ , high  $V_d$ ), and that an optimal force interaction range may exist; this is revisited in Chapter 4.

### 3.3 Precision

The metrics  $C_v$  and  $RMS_n$  are indicators of human velocity-control precision. The raw data for  $C_v$  and  $RMS_n$  are shown in Figure 3.7 and Figure 3.8, respectively. The precision metrics quantify variation about the mean velocity, which can be thought of as tremor. Therefore, Figure 3.7 and Figure 3.8 show the variation in the amount of tremor for each combination of  $V_d$  and  $k_a$ . Similar to the results shown by the accuracy metrics, there is substantially more variation in precision for trials conducted with a desired velocity of 0.1 mm/s than for trials conducted with faster desired velocities.

The metric  $C_v$  quantified precision in terms of the standard deviation of velocity normalized by the mean velocity. The effect of  $V_d$  was significant,  $F(3,2534) = 5032.753$ ,  $p < 0.001$ , as was the effect of  $k_a$ ,  $F(3,2534) = 116.888$ ,  $p < 0.001$ , in a model of  $C_v$  that included  $k_a$ ,  $V_d$ , and the  $k_a$ -by- $V_d$  interaction; the interaction was also significant,  $F(9,2534) = 15.929$ ,  $p < 0.001$ . Figure 3.9a shows that as  $V_d$  increases from 0.1 mm/s,  $C_v$  decreases asymptotically for all  $k_a$  values. The most significant improvement in  $C_v$  occurs when increasing  $V_d$  from 0.1 to 0.4 mm/s. This improvement is also clearly shown in Figure 3.9b.

This correlates to the results found for  $E_d$ , which show that subjects performed most

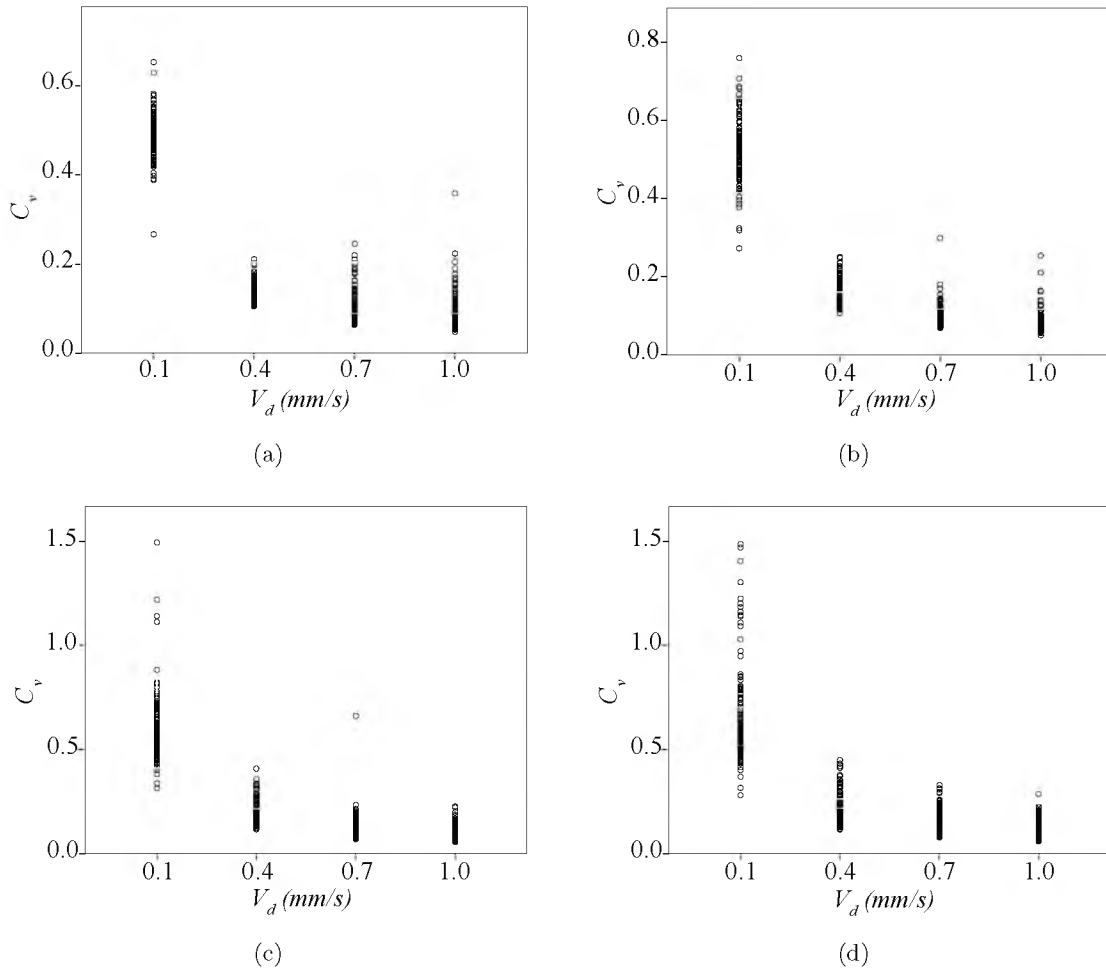


**Figure 3.7:** Raw data for metric  $C_v$  for all ten subjects by admittance gain: (a)  $k_a = 0.1$ , (b)  $k_a = 0.4$ , (c)  $k_a = 0.7$ , and (d)  $k_a = 1.0$ .

poorly during trials that had a very low  $V_d$  (0.1 mm/s). It can easily be seen that, at low values of  $V_d$ , the precision is much more sensitive to changes in  $V_d$  than it is to changes in  $k_a$ , and at higher values of  $V_d$ , the effect of  $V_d$  and  $k_a$  on precision become comparable. It can also be seen that the best precision occurs at combinations of high  $V_d$  and low  $k_a$ , which correspond to large applied force.

The metric  $RMS_n$  shows results that are very similar to those of  $C_v$ . Figure 3.10a shows the relationship between  $RMS_n$  and  $V_d$  for all values of  $k_a$ . The same data are shown in Figure 3.10b only the data show the relationship between  $RMS_n$  and  $k_a$  for all values of  $V_d$ . The trend shown in Figure 3.10a is nearly identical to the trend in Figure 3.9a.

The effect of  $V_d$  was significant,  $F(3,2535) = 1859.259$ ,  $p < 0.001$ , as was the effect of  $k_a$ ,  $F(3,2535) = 64.962$ ,  $p < 0.001$ , in a model of  $RMS_n$  that included  $k_a$ ,  $V_d$ , and the  $k_a$ -by- $V_d$  interaction; the interaction was also significant,  $F(9,2535) = 26.786$ ,  $p < 0.001$ . The  $RMS_n$

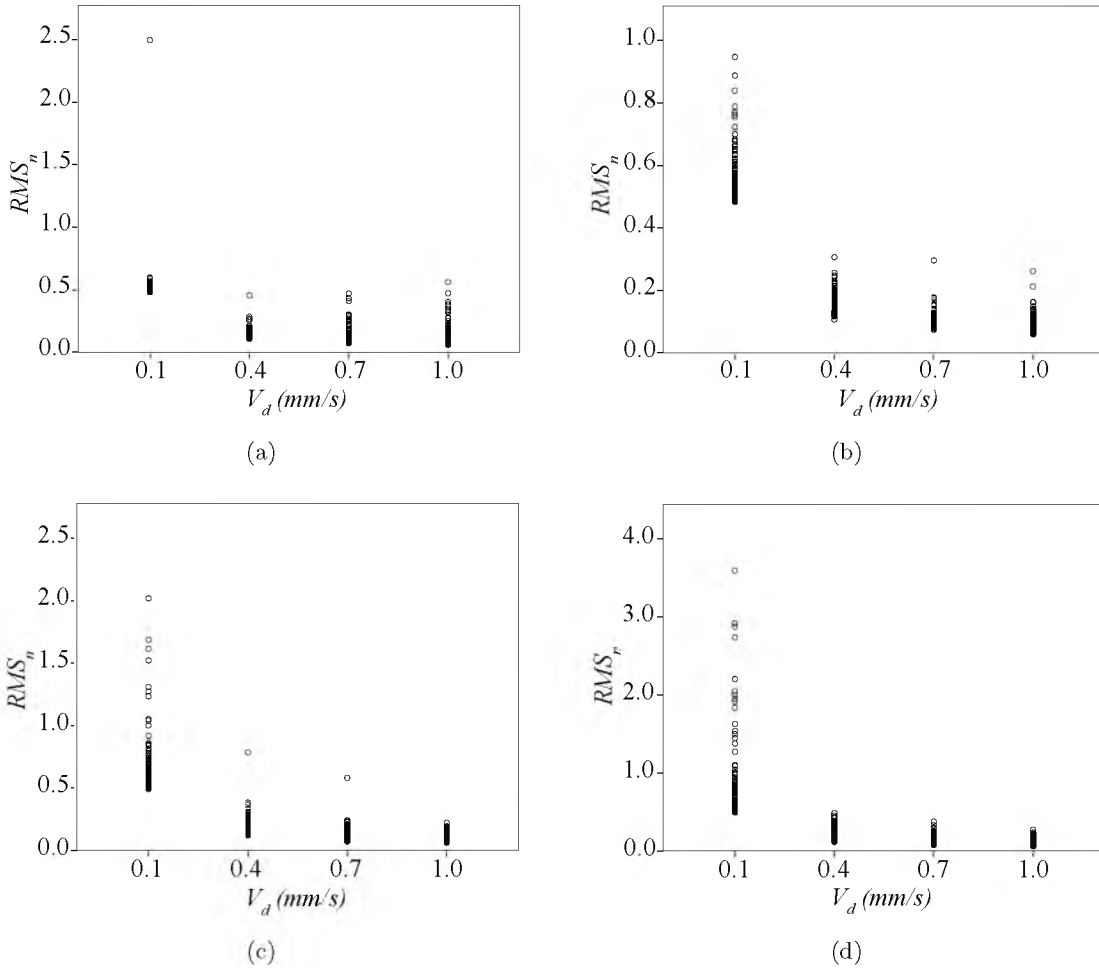


**Figure 3.8:** Raw data for metric  $RMS_n$  for all ten subjects by admittance gain: (a)  $k_a = 0.1$ , (b)  $k_a = 0.4$ , (c)  $k_a = 0.7$ , and (d)  $k_a = 1.0$ .

and  $C_v$  metrics have nearly identical trends because they both evaluate velocity-control precision. The difference between the two metrics is very slight:  $RMS_n$  considers the variation from the desired velocity while  $C_v$  considers the variation from the subject's mean velocity. Since  $RMS_n$  does not give any additional insight into human velocity-control precision,  $C_v$  is deemed more meaningful because it quantifies precision (which can also be thought of as tremor) independent of the velocity level.  $C_v$  is truly a measurement of the subject's physical limitations in maintaining a constant velocity. In some sense,  $RMS_n$  can be thought of as the same precision information present in  $C_v$ , but corrupted by inaccuracy.

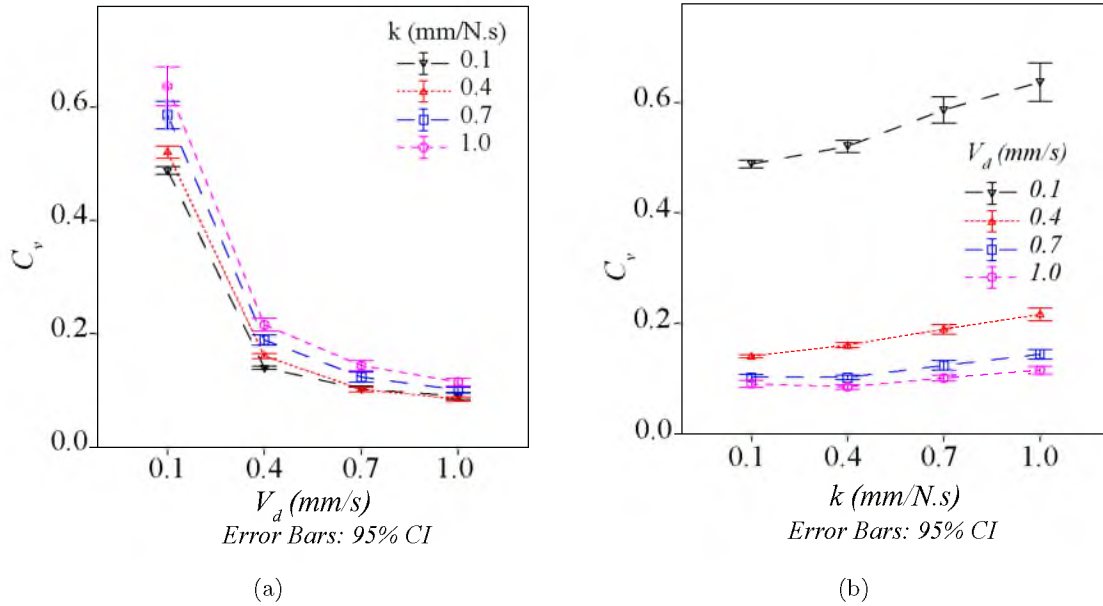


**Figure 3.9:** Experimental results for metric  $C_v$  for all 10 subjects combined.  $C_v$  is a measure of the subject's ability to maintain a constant velocity normalized by the subject's mean velocity, as defined in (2.7). (a) shows  $C_v$  across all  $V_d$  values at different levels of  $k_a$ , and (b) shows  $C_v$  across all  $k_a$  values at different levels of  $V_d$ .

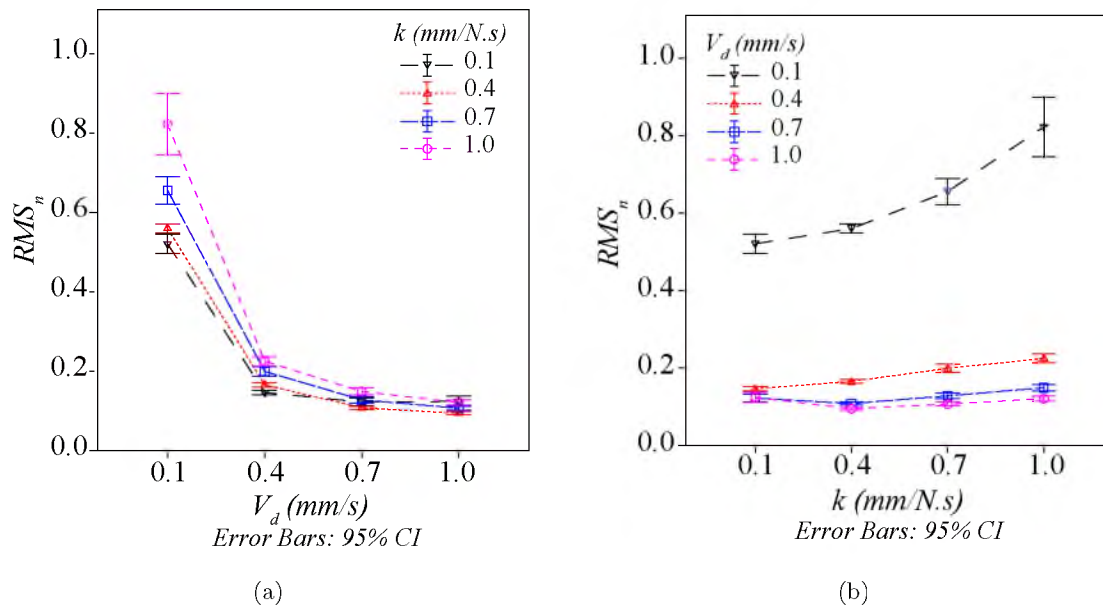


**Figure 3.10:** Experimental results for metric  $RMS_n$  for all 10 subjects combined.  $RMS_n$  is a measure of the subject's velocity variation from the desired velocity, as defined in (2.8). (a) shows  $RMS_n$  across all  $V_d$  values at different levels of  $k_a$ , and (b) shows  $RMS_n$  across all  $k_a$  values at different levels of  $V_d$ .

## CHAPTER 4

### DISCUSSION

Human velocity-control performance was described in terms of accuracy and precision. The results of our statistical analysis show that both admittance gain ( $k_a$ ) and desired velocity ( $V_d$ ) are significant predictors of human velocity-control performance. The scale factor ( $S$ ) tested in this study was shown to be insignificant in determining human velocity-control performance in the vast majority of cases considered. This magnification between the device motion and the visual display only had an effect for the two cases where the visual velocity, which was observed on the visual display, was less than approximately 5 mm/s. Otherwise, the scale factor does not affect human velocity-control performance for the range of admittance gains, velocities, and scaling factors considered in this experiment. Recall, however, that accuracy in all cases herein is normalized by the target velocity, which in this case is a very small number, so results should be interpreted in light of this fact. According to [17], human performance in positioning tasks is highly dependent on the scale factor. As such, where positioning performance is relevant, the scale factor can be selected to optimize positioning performance without diminishing velocity-control performance. However, a computer mouse is not an admittance-type device, so direct comparisons of our results to [7] should be made with caution.

This experiment focused on a range of relatively slow velocities (0.1, 0.4, 0.7, 1.0 mm/s). This range of velocities is appropriate for this experiment since we are primarily interested in applications that require high precision and accuracy and therefore operate at relatively low velocities. Muñoz et al. [17] assert that humans do not have precise positioning control when the velocity of a movement exceeds a threshold velocity value. Although there are no data that directly correlate the positioning experiment of [17] with velocity tracking performance of this experiment, it is important to note that the current work does not consider high speed movements that would exceed the threshold velocity were human-control performance is known to degrade. As such, the results of this experiment should not be extrapolated, since the effects of  $V_d$  and  $k_a$  may not follow the same trends at higher velocities.

The metric  $E_d$  was a measure of how accurately a subject tracked the desired velocity. Figure 3.5 shows the experimental results for  $E_d$  across all 10 subjects, where an  $E_d$  value of zero denotes perfect accuracy.  $E_d$  is a signed metric and is sensitive to the direction of the error in accuracy, meaning that  $E_d$  can differentiate if the subject erred by moving too fast or too slowly. The metric  $E_d$  shows that on average, for  $V_d$  equal to 0.1 mm/s, the subjects' actual velocity was consistently faster than  $V_d$ . In contrast, the subjects' average velocity were slower than  $V_d$  for all other levels of  $V_d$  tested here. Therefore, it seems that there exists a threshold velocity between 0.1 mm/s and 0.4 mm/s where subjects would theoretically perform perfectly. In some situations it may be optimal to set the admittance gain such that operators tend to err by moving slower than the desired velocity, instead of erring by moving too fast, but it is likely that that ultimate goal would be to perfectly track the desired velocity. Table 3.1 lists  $V_d$  values for each  $k_a$  value that, theoretically, on average, result in optimal accuracy. A  $V_d$  value that is higher or lower than the  $V_d$  reported in Table 3.1 will result in an average velocity that is slower or faster than the desired velocity, respectively. Insuring that  $V_d$  remains above these threshold  $V_d$  values increases the likelihood that an operator will err by moving too slowly, in the event that the operator does err. Setting the admittance gain  $k_a$  of the device such that operators tend to move too slowly could reduce the risk of overshooting a target, making the device safer to operate.

Nambi et al. [9] reported similar results for tests that were conducted using a stationary device. Subjects were told to maintain a constant force on the device for a period of 2 seconds while the applied force was recorded. They observed that subjects had a tendency to apply forces higher than the target force at target forces below approximately 2 N, and to apply forces lower than the target force at target forces higher than 2 N. Therefore, a force level of 2 N seems to be a threshold force where average performance was the best, for the stationary tests.

The results of the current work show that the threshold force level, which results in the theoretical best velocity-control performance, changes as a result of the motion of the admittance-type device. Table 3.1 shows the best force levels that correspond to each admittance gain and respective best velocity, according to (1.1). For an admittance gain of 0.1 mm/(N·s) the best velocity is 0.27 mm/s and the corresponding best force is 2.7 N. This force was calculated using an estimate of the best velocity determined by linearly interpolating points on a trend that is not linear. Using a nonlinear interpolation would result in an best force level that is slightly smaller than 2.7 N, bringing it closer to the

threshold force level reported by Nambi et al. [9] for the isometric force-control tests conducted on a static device. Nambi et al. also reported that for an admittance gain of  $0.1 \text{ mm}/(\text{N}\cdot\text{s})$ , subjects' force-control performance while operating an admittance-type device under control law (1.1) was nearly the same as the force-control performance recorded on a static device. Therefore, it is not surprising that for an admittance gain equal to  $0.1 \text{ mm}/(\text{N}\cdot\text{s})$  the best force is nearly the same as the best force level for the static case. Nambi et al. also report that as the admittance gain is increased the user's performance quickly becomes dissimilar from the static case. It seems plausible that as the admittance gain increases the best force level also changes from that of the static case.

Figure 4.1 shows the best force levels for each admittance gain, as reported in Table 3.1. The trend shows that the best force level reduces asymptotically towards  $0.4 \text{ N}$  as the admittance gain increases toward  $1.0 \text{ mm}/\text{N}\cdot\text{s}$ . Figure 4.2 shows the best force levels that correspond to each best velocity level, according to Table 3.1. This trend shows that the best force level decreases as the desired velocity increases. Both of these trends show that the best force level for an admittance-type device, controlled under control law (1.1), is smaller than the best force level determined by the static force measurements in [9]. Figure 4.3 shows the best admittance gain for each target velocity; this presentation of data is the most constructive, in that it provides a recommendation for the best choice of admittance gain to set if there is knowledge of the type of velocities expected for a given task.

It is important to note that the  $k_a$ - $V_d$  pairs that are being reported as "best" values in Table 3.1 do give a sense of the best operating conditions, but do not represent equally good performance. Instead, the best velocity simply maximizes the performance attainable for a given admittance gain. Furthermore, the best velocity is only the best on average and serves as only an indication of the point at which subjects tend not to lead or lag the desired velocity in the aggregate. These results are only useful in understanding if the subject is more likely to move too fast or too slowly, and gives no indication of how often and how much the subject will err.

The variation from the mean of  $E_d$  is in a sense a better indicator of velocity-control accuracy because it indicates how often the subjects erred during the trials. Table 4.1 shows the variance in  $E_d$  for all combinations of  $k_a$  and  $V_d$ . The variance in  $E_d$  was the highest for trials that had a  $V_d$  equal to  $0.1$ , all other values of  $V_d$  had variance levels that were smaller by about an order of magnitude in many cases. In addition to having high levels of variance, trials with a  $V_d$  of  $0.1$  had the largest mean  $E_d$ , which means that subject's average accuracy was poor for these trials, as shown in Figure 3.6. These results show that

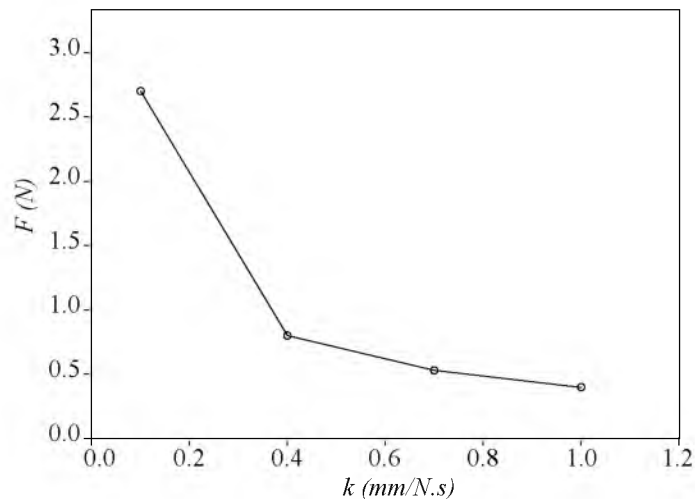


**Figure 4.1:** Best force level in terms of accuracy for each admittance gain that was tested, as reported in Table 3.1.

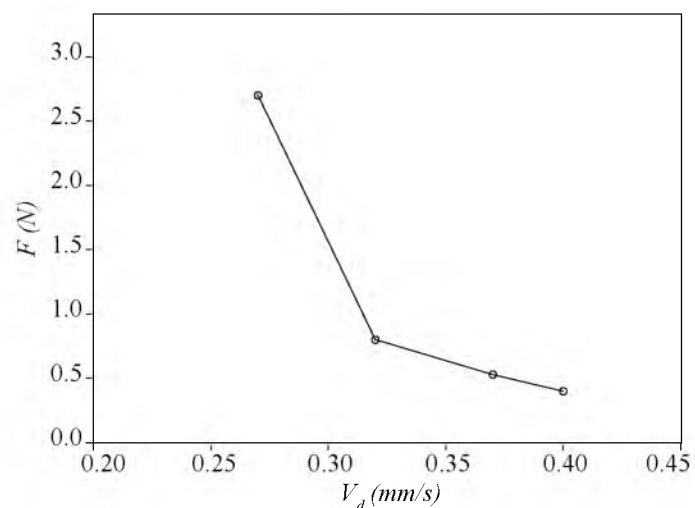


**Figure 4.2:** Best force level in terms of accuracy for each desired velocity that was tested, as reported in Table 3.1.

human velocity-control accuracy degrades significantly as a result of reducing the desired velocity to 0.1 mm/s.

Nambi et al. [9] state that there is likely a range of forces and velocities within which humans optimally interact with admittance-type devices. A  $V_d$  of 0.1 mm/s appears to be outside the range of velocities that results in optimal performance, at least when considering velocity-control accuracy. Nambi et al. also concluded that the force level is the most important factor to consider when choosing the best value for the admittance gain. They

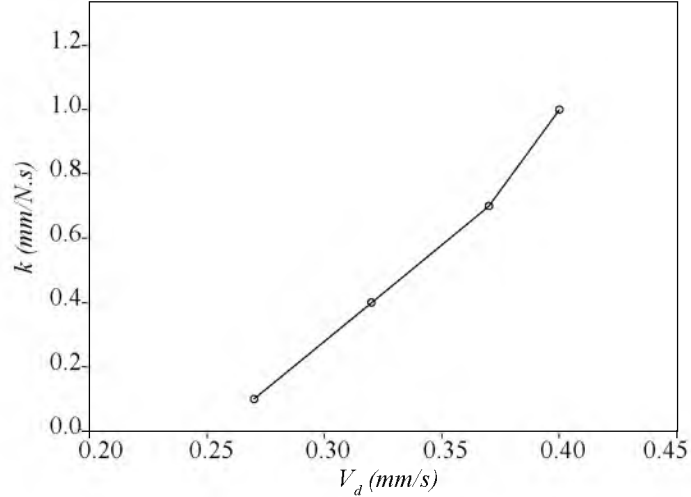


**Figure 4.3:** Best admittance gain in terms of accuracy for each desired velocity that was tested, as reported in Table 3.1.

**Table 4.1:** Variance in  $E_d$  across all subject for each  $V_d$  and  $k_a$  combination. Variance was highest when  $V_d$  was equal to 0.1 mm/s (highlighted in gray)

$V_d \backslash k_a$	0.1	0.4	0.7	1.0
0.1	0.039	0.027	0.052	0.175
0.4	0.003	0.003	0.007	0.004
0.7	0.005	0.001	0.002	0.002
1.0	0.008	0.001	0.001	0.001

reported that human force-control precision degrades significantly for target forces below 0.5 N. Results from the current work show that a force of 0.4 N is an acceptable force level and that variation in accuracy is excessive for force levels below 0.4 N. It is possible that Nambi et al. did not detect that 0.4 N is an acceptable force level because they did not explicitly test 0.4 N (Their test force levels included 0.56 N and 0.32 N but not 0.4 N). Table 2.2 shows that three of the four target forces are below 0.4 N for trials that had  $V_d$  equal to 0.1 mm/s. Therefore, it is likely that the very low force level is the main cause of poor accuracy; however, it also appears that the low velocity is also contributing to poor accuracy independent of force. A clear example of this is shown by the trials that had a  $V_d$  equal to 0.1 mm/s and a  $k_a$  value equal to 0.1 mm/(N.s). The target force for these trials was 1.0 N, according to (1.1). This force level is above the threshold force of 0.4 N and should, therefore, result in good accuracy if we consider only the effects of force. Furthermore, other trials that had a target force of 1.0 N, but had a  $V_d$  value larger than 0.1, resulted in good

accuracy. However, when  $V_d$  is set equal to 0.1 mm/s the variation in  $E_d$  is high, showing that accuracy is poor under these circumstances, regardless of whether the force level is optimal. In this example the force falls within the range of optimal forces, but the desired velocity does not fall within the optimal range of velocities, which results in suboptimal accuracy (see Figure 3.9a).

The metric  $E_a$  is the absolute values of the metric  $E_d$  and, therefore, shows the accuracy in absolute terms. Instead of quantifying the accuracy error in terms of moving too fast or too slowly,  $E_a$  shows the absolute magnitude of the accuracy error for all trials. The mean of  $E_a$  gives a true sense of the overall accuracy error because it shows the subjects' true divergence from perfect accuracy. Therefore, the mean of  $E_a$  is a better overall indicator of accuracy across all trials and operating conditions than is the mean of  $E_d$ . Figure 3.6a shows the experimental results for metric  $E_a$ , where an  $E_a$  of zero indicates perfect accuracy. The mean  $E_a$  values are shown in Table 4.2 and values that seem to be relatively high are highlighted in gray. The value at which the mean is considered to be high is somewhat arbitrary, and was selected based on visual inspection of Figure 3.6a. A different value that is more or less conservative may be appropriate for different applications.

Trials that had high variance in  $E_d$  also had large mean  $E_a$ . This is expected because data with high variance correlates to a large mean for the absolute metric  $E_a$ . This can be seen in Figure 3.4, which shows the raw data for the metric  $E_a$ . It is apparent that the mean value of  $E_a$  is larger for data sets with high variance. This shows that the mean of  $E_a$  must be high when the variance of  $E_d$  is high. This occurs when trials have a target force or desired velocity that is too low, which shows that humans may not have adequate motor skills to accurately control velocity at such low speeds and forces, at least not consistently. It is not clear whether the low target force or the low desired velocity has the most degrading effect on accuracy; however, as was shown above, both do contribute to poor accuracy.

So far we have seen that the desired velocity and target force need to be above their respective thresholds to maximize accuracy. In part, this can be accomplished by calibrating the admittance-type device such that there would be very little variation in  $E_d$  and the mean  $E_a$  would be small. Initially, it seems that the variation on  $E_d$  and the mean  $E_a$  values are redundant indicators of accuracy; however, both do give different insight into accuracy error. The variation in  $E_d$  is an indicator of consistency, while the mean  $E_a$  is a measure of how accurate subject actually were, on average. Further inspection of Table 4.1 and Table 4.2 shows that some trials have low variance in  $E_d$  but still have large mean  $E_a$ . The lack of variance in  $E_d$  shows that subjects are consistent, but the large mean  $E_a$  shows that they

**Table 4.2:** Mean  $E_a$  for each  $V_d$  and  $k_a$  combination, as shown in Figure 3.6. Values that are relatively high are highlighted in gray.

$V_d \backslash k_a$	0.1	0.4	0.7	1.0
0.1	0.079	0.115	0.150	0.253
0.4	0.044	0.041	0.054	0.052
0.7	0.065	0.038	0.040	0.043
1.0	0.081	0.042	0.039	0.042

are inaccurate. As an example, test subjects were consistently inaccurate for trials that had a  $V_d$  of 1.0 mm/s, a  $k_a$  of 0.1 mm/N·s, and a target force of 10 N. A velocity of 1.0 mm/s is within the optimal range of velocities for all other relevant trials, but the mean  $E_a$  is still high. The target force of 10 N is likely the cause of inaccuracy in this case. Subjects consistently applied a force that was too low and never accurately attained the desired velocity.

It appears that accuracy degrades when the target force is too high or too low. Table 4.3 shows the forces that correspond to each combination of  $k_a$  and  $V_d$  that was used in the experiment. Forces that correspond to trials with large mean  $E_a$  are highlighted in gray. Based on the values shown in Table 4.3, accuracy is optimal when the target force is in the range of 0.4 N to 4.0 N, inclusive. Furthermore, accuracy is optimal when the desired velocity is between 0.4 mm/s and 1.0 mm/s, inclusive. The admittance gain plays an important role because it must be selected such that the desired velocity and target force remain within their respective optimal ranges simultaneously.

The coefficient of variance in velocity,  $C_v$ , quantifies human velocity-control precision, or the subject's ability to stably maintain some mean velocity; a  $C_v$  of zero correlates to perfect precision. Statistical analysis of  $C_v$  showed that precision is significantly affected by both  $k_a$  and  $V_d$  for all trials. Figure 3.9a shows that  $C_v$  improves asymptotically as  $V_d$  increases from 0.1 mm/s. Similar to the accuracy metric,  $C_v$  is very high for a  $V_d$  of 0.1 mm/s, showing that precision is poor for a  $V_d$  of 0.1 mm/s. Therefore, it is clear that human velocity-control precision is, in general, poor for relatively slow velocities.

To maximize velocity-control performance one must consider both accuracy and precision. Optimizing performance for both accuracy and precision requires that the desired velocity and target force remain above a threshold value. The minimum velocity threshold value and the minimum force threshold value were found to be about 0.4 mm/s and 0.4 N, respectively, for both accuracy and precision. To optimize accuracy the target force must also be constrained by a maximum force threshold value, which was found to be about

**Table 4.3:** Target force levels (N) determined according to (1.1) for each level of  $V_d$  (mm/s) and  $k_a$  (mm/(N·s)) used in the experiment. Force levels highlighted in gray correspond to trials that had poor accuracy (high mean  $E_a$ ), as seen in Table 4.2 and Figure 3.6.

$V_d \backslash k_a$	0.1	0.4	0.7	1.0
0.1	1.0	0.25	0.14	0.1
0.4	4.0	1.0	0.57	0.4
0.7	7.0	1.75	1.0	0.7
1.0	10.0	2.5	1.43	1.0

4.0 N. Precision, on the other hand, does not have a maximum force threshold. This result is intuitive since the precision metric is in terms of percentage error. At very low forces a subject’s tremor would apply uncontrolled, undesired forces on the sensor that are on the same order of magnitude as the target force. When the force is increased the variation in human force-control is reduced ([14, 15]); therefore, tremor and other such disturbances have little effect on the precision measurement for larger force levels, since the variation in force is small in comparison to the target force.

If the desired velocity and target force are above their threshold values, then the admittance gain has the most influence on velocity-control precision. Figure 3.9a shows that precision was better for trials that implemented lower admittance gains. Based on control law (1.1), lower admittance gains correlate to higher target force for a given velocity. In fact, the best precision occurred for the highest velocity (1.0 mm/s) and lowest admittance gain (0.1 mm/s), which correlate to the highest force level (10 N). Although this force level is optimal for precision, accuracy degrades when the force level is larger than its maximum threshold of 4.0 N.

In this case the subject’s force application variation is minimal due to the high target force; however, the subjects did not apply a force that was high enough to attain the desired velocity. This result can only be understood by looking at both  $C_v$  and  $E_a$  together, because they give different information about velocity-control performance.  $C_v$  only considers the variation of the actual velocity from the mean velocity and ignores how close the mean velocity is to the desired velocity. If there was little variance in the subject’s velocity,  $C_v$  would detect good performance, even if the actual velocity was half that of the desired velocity. On the other hand,  $E_a$  ignores the variation in the subject’s velocity and only compares the deviance of the mean velocity from the desired velocity.

There must be some compromise when optimizing accuracy and precision. Optimal accuracy can be attained for only a limited range of forces and velocities, while optimal precision can be attained for larger forces. However, it is not practical to increase the

target force very much to gain better precision, since the user would lag behind the desired velocity and become fatigued during operation of the device. Furthermore, the range of forces and velocities that result in optimal accuracy also result in good precision, making accuracy a more conservative criteria for optimizing velocity-control performance.

Although the admittance gain is a significant predictor of precision and accuracy, the target force level and the desired velocity are the most important factors to consider when configuring an admittance-type device. The admittance gain should be selected for a given application to ensure that the velocity and force at the point of contact between the user and the robotic device remain within their optimal range. It seems somewhat unfortunate that, during the normal course of operation of an admittance-type robot, the user will start and stop at rest, and must therefore pass through the low-velocity range where control is worst. However, it should be recalled that all metrics used herein were normalized nominal values, so while the percentage errors may be large in the low-velocity range, the absolute errors will still be small.

## CHAPTER 5

### CONCLUSION

In this thesis we have studied the effects of velocity ( $V_d$ ), admittance gain ( $k_a$ ), and scale factor ( $S$ ) on human velocity-control accuracy and precision when using admittance-type devices. The experiment was also conducted to determine under which operating conditions human-velocity control is optimized for admittance devices that are controlled under proportional-velocity control, and to determine the degradation in control under non-optimal conditions. This study was also conducted to determine the effect that visual position/velocity feedback has on human velocity control of an admittance-type device. Specifically, we wanted to know if scaling the visual velocity feedback had any effect on human-velocity control performance.

We give evidence that there exists a range of velocities and forces within which humans optimally interact with admittance-type devices. We found that human-velocity control accuracy and precision are poor when the desired velocity is very low (below 0.4 mm/s) or the target force is very low (below 0.4 N). To ensure a high level of control over the device the desired velocity should be above 0.4 mm/s and the force should be above 0.4 N. Additionally, we found that accuracy degrades when the target force is very large (above 4.0 N). These values seem to indicate that humans do not have adequate motor skills to accurately and precisely control velocity at speeds and forces that are either too low or too high, at least not consistently. We found that the optimal range of velocities is between 0.4 mm/s and 1.0 mm/s, inclusive, and the optimal range of forces is between 0.4 N and 4.0 N, inclusive. To ensure optimal velocity-control performance, the admittance gain should be selected such that the desired velocity and target force remain within their respective optimal ranges simultaneously.

We also found that on average subjects moved faster than the desired velocity when the desired velocity was 0.1 mm/s and subjects were slower than the desired velocity when it was higher than 0.4 mm/s. For each admittance gain there is a different threshold velocity, which was determined experimentally in this study. If the device operates at a

velocity that is faster than the threshold velocity the operator will tend to lag the desired velocity. Conversely, if the device operates at a velocity slower than the threshold velocity the operator will tend to lead the desired velocity.

We found that in velocity-tracking tasks, scaling the visual velocity feedback has no effect on precision and has a very limited effect on accuracy, for the range of velocities tested here. It was determined that the effect of the scale factor was negligible when compared to the effects of  $V_d$  and  $k_a$ . The scale factor was, therefore, deemed negligible in determining velocity-tracking performance. However, others have shown that the scale factor has a significant effect on performance during positioning tasks. Therefore, the scaling factor should be selected to optimize positioning performance, knowing that velocity-tracking performance will not be affected by the scale factor.

Humans are not capable of performing manipulation tasks precisely or accurately when the manipulation velocity or force are too small. When an admittance-type device is used to enhance human manipulation performance, the workspace is essentially enlarged to a size that is optimal for human performance. Likewise, the velocities and forces can be scaled such that humans can perform manipulation tasks accurately and precisely. This research shows that the admittance gain should be selected such that the manipulation velocities and forces are within their optimal ranges.

## REFERENCES

- [1] Adams, R. J., and Hannaford, B., 1999. “Stable haptic interaction with virtual environments.” *IEEE Trans. Robotics and Automation*, **15**(3), pp. 465–474.
- [2] Uñeri, A., Balicki, M. A., Handa, J., Gehlbach, P., Taylor, R. H., and Iordachita, I., 2010. “New steady-hand eye robot with micro-force sensing for vitreoretinal surgery.” In *IEEE Int. Conf. Biomedical Robotics and Biomechatronics*, pp. 814–819.
- [3] Mitchell, B., John Koo, M., Iordachita, I., Kazanzides, P., Kapoor, A., James Hunda, M., Hager, G., and Taylor, R., 2007. “Development and application of a new steady-hand manipulator for retinal surger.” In *Proc. IEEE Int. Conf. Robotics and Automation*, pp. 623–629.
- [4] Taylor, R., Jensen, P., Whitcomb, L., Barnes, A., Kumar, R., Stoianovici, D., Gupta, P., Wang, Z., deJuan deJuan deJuan, E., and Kavoussi, L., 1999. “Steady-hand robotic system for microsurgical augmentation.” *Int. J. Robotics Research*, **18**(12), pp. 1201–1210.
- [5] Fehlbberg, M. A., Gleeson, B. T., and Provancher, W. R., 2012. “Active handrest: A large workspace tool for precision manipulation.” *The International Journal of Robotics Research*, **31**(3), pp. 289–301.
- [6] Fehlbberg, M., King, R., Doxon, A., and Provancher, W., 2012. “Evaluation of active handrest performance using labyrinths with adaptive admittance control and virtual fixtures.” In *IEEE Haptics Symposium*, pp. 273–280.
- [7] Fehlbberg, M. A., Gleeson, B. T., Leishman, L. C., and Provancher, W. R., 2010. “Active handrest for precision manipulation and ergonomic support.” In *Proc. Symp. Haptic Interfaces for Virtual Environments and Teleoperator Systems*, pp. 489–496.
- [8] Fehlbberg, M., Gleeson, B., and Provancher, W., 2010. “Analysis of active handrest control methods.” In *Haptics: Generating and Perceiving Tangible Sensations*, A. Kappers, J. van Erp, W. Bergmann Tiest, and F. van der Helm, eds., Vol. 6191 of *Lecture Notes in Computer Science*. Springer Berlin / Heidelberg, pp. 326–331.
- [9] Nambi, M., Provancher, W. R., and Abbott, J. J., 2011. “On the ability of humans to apply controlled forces to admittance-type devices.” *Advanced Robotics*, **25**, pp. 629–650.
- [10] Jones, L. A., 2000. “Visual and haptic feedback in the control of force.” *Experimental Brain Research*, **130**, pp. 269–272.
- [11] Srinivasan, M. A., and Chen, J., 1993. “Human performance in controlling normal forces of contact with rigid objects.” In *Proc. ASME Dynamic Systems and Control Division: Advances in Robotics, Mechatronics, and Haptic Interfaces*, pp. 119–125.

- [12] Allin, S., Matsuoka, Y., and Klatzky, R., 2002. “Measuring just noticeable differences for haptic force feedback: Implications for rehabilitation.” In Proc. Symp. Haptic Interfaces for Virtual Environments and Teleoperator Systems, pp. 299–302.
- [13] Lederman, S. J., Howe, R. D., Klatzky, R. L., and Hamilton, C., 2004. “Force variability during surface contact with bare finger or rigid probe.” In Proc. Symp. Haptic Interfaces for Virtual Environments and Teleoperator Systems, pp. 154–160.
- [14] Hamilton, A. F. C., Jones, K. E., and Wolpert, D. M., 2004. “The scaling of motor noise with muscle strength and motor unit number in humans.” *Experimental Brain Research*, **157**, pp. 417–430.
- [15] Taylor, A. M., Christou, E. A., and Enoka, R. M., 2003. “Multiple features of motor-unit activity influence force fluctuations during isometric contractions.” *J Neurophysiol*, **90**(2), pp. 1350–1361.
- [16] Wu, M., Abbott, J. J., and Okamura, A. M., 2005. “Effect of velocity on human force control.” In Proc. Joint Eurohaptics Conf. and Symp. Haptic Interfaces for Virtual Environment and Teleoperator Systems, pp. 73–79.
- [17] L. M. Muñoz, A. Casals, M. F., and Amat, J., 2011. “Motor-model-based dynamic scaling in human-computer interfaces.” *IEEE Trans. Systems, Man, and Cybernetics*, **41**(2), pp. 435–447.
- [18] Fitts, P., 1954. “The information capacity of the human motor system in controlling the amplitude of movement.” *J. Experimental Psychology*, **47**(6), pp. 381–391.
- [19] CHAI 3D: The open source haptics project <http://www.chai3d.org/>.